32 Kim WJ, Kang YJ, Koh EM, Ahn KS, Cha HS, Lee WH. LIGHT is involved in the pathogenesis of rheumatoid arthritis by inducing the expression of pro-inflammatory cytokines and MMP-9 in macrophages. *Immunology* 2005; **114**:272–9.

33 Kang YM, Kim SY, Kang JH, Han SW, Nam EJ, Kyung HS, Park JY, Kim IS. LIGHT up-regulated on B lymphocytes and monocytes in rheumatoid arthritis mediates cellular adhesion and metalloproteinase production by synoviocytes. *Arthritis Rheum* 2007; **56**:1106–17.

34 Pierer M, Brentano F, Rethage J, Wagner U, Hantzschel H, Gay RE, Gay S, Kyburz D. The TNF superfamily member LIGHT contributes to survival and activation of synovial fibroblasts in rheumatoid arthritis. *Rheumatology (Oxford)* 2007; **46**:1063–70.

35 Nakamura I, Takahashi N, Sasaki T, Jimi E, Kurokawa T, Suda T. Chemical and physical properties of the extracellular matrix are required for the actin ring formation in osteoclasts. *J Bone Miner Res* 1996; **11**:1873–9.

36 Tsuboi H, Matsui Y, Hayashida K *et al.* Tartrate resistant acid phosphatase (TRAP) positive cells in rheumatoid synovium may induce the destruction of articular cartilage. *Ann Rheum Dis* 2003; **62**:196–203.

37 Hayashida K, Nanki T, Girschick H, Yavuz S, Ochi T, Lipsky PE. Synovial stromal cells from rheumatoid arthritis patients attract monocytes by producing MCP-1 and IL-8. *Arthritis Res* 2001; **3**:118–26.

38 Lee WH, Kim SH, Lee Y, Lee BB, Kwon B, Song H, Kwon BS, Park JE. Tumor necrosis factor receptor superfamily 14 is involved in atherogenesis by inducing proinflammatory cytokines and matrix metalloproteinases. *Arterioscler Thromb Vasc Biol* 2001; **21**:2004–10.

39 Edwards JR, Sun SG, Locklin R, Shipman CM, Adamopoulos IE, Athanasou NA, Sabokbar A. LIGHT (TNFSF14), a novel mediator of bone resorption, is elevated in rheumatoid arthritis. *Arthritis Rheum* 2006; **54**:1451–62.

40 Hou P, Troen T, Ovejero MC *et al.* Matrix metalloproteinase-12 (MMP-12) in osteoclasts: new lesson on the involvement of MMPs in bone resorption. *Bone* 2004; **34**:37–47.

41 Liu M, Sun H, Wang X *et al.* Association of increased expression of macrophage elastase (matrix metalloproteinase 12) with rheumatoid arthritis. *Arthritis Rheum* 2004; **50**:3112–7.

42 Wang X, Liang J, Koike T *et al.* Overexpression of human matrix metalloproteinase-12 enhances the development of inflammatory arthritis in transgenic rabbits. *Am J Pathol* 2004; **165**:1375–83.

43 Janusz MJ, Hare M, Durham SL, Potempa J, McGraw W, Pike R, Travis J, Shapiro SD. Cartilage proteoglycan degradation by a mouse transformed macrophage cell line is mediated by macrophage metalloelastase. *Inflamm Res* 1999; **48**:280–8.

44 Hautamaki RD, Kobayashi DK, Senior RM, Shapiro SD. Requirement for macrophage elastase for cigarette smoke induced emphysema in mice. *Science* 1997; **277**:2002–4.

45 Vaalamo M, Kariniemi AL, Shapiro SD, Saarialho-Kere U. Enhanced expression of human metalloelastase (MMP-12) in cutaneous granulomas and macrophage migration. *J Invest Dermatol* 1999; **112**:499–505.

46 Adamopoulos IE, Sabokbar A, Wordsworth BP, Carr A, Ferguson DJ, Athanasou NA. Synovial fluid macrophages are capable of osteoclast formation and resorption. *J Pathol* 2006; **208**:35–43.

47 Hirayama T, Danks L, Sabokbar A, Athanasou NA. Osteoclast formation and activity in the pathogenesis of osteoporosis in rheumatoid arthritis. *Rheumatology (Oxford)* 2002; **41**:1232–9.

Involvement of a disintegrin and metalloproteinase 10 and 17 in shedding of tumor necrosis factor-α

Atsuhiko Hikita, Nobuho Tanaka, Shoji Yamane, Yasuko Ikeda, Hiroshi Furukawa, Shigeto Tohma, Ryuji Suzuki, Sakae Tanaka, Hiroyuki Mitomi, and Naoshi Fukui

Abstract: Tumor necrosis factor-α (TNF-α) is initially synthesized as a membrane-bound protein and converted into a soluble form by proteolytic cleavage. Although a disintegrin and metalloproteinase 17 (ADAM17) is considered to be the primary sheddase for TNF-α, it is not known whether ADAM17 is solely responsible for that process in any type of cells. To identify the TNF-α sheddase(s) in varieties of cells, we performed experiments using a unique screening system and observed that ADAM9, ADAM10, ADAM17, and ADAM19 were capable of cleaving TNF-α. We then performed RNA interference experiments and confirmed that ADAM10 and ADAM17 were in fact involved in TNF-α shedding in 293A cells. In mouse macrophages, ADAM17 was confirmed to be the primary sheddase, but the involvement of ADAM10 was also demonstrated. In NIH3T3 cells, ADAM10 could be more important in the shedding than ADAM17. In mouse vascular endothelial cell line UV-2, ADAM10 and ADAM17 were equally involved in TNF-α shedding, whereas ADAM17 was a major sheddase in human osteoarthritic chondrocytes. From these observations and others, we concluded that both ADAM10 and ADAM17 can be a TNF-α sheddase and that their significance could be determined by their expression levels and the abundance of tissue inhibitor of metalloproteinases.

Key words: TNF-α, ADAM10, ADAM17, TIMP, ectodomain shedding.

Résumé : Le TNF-α est d'abord synthétisé sous forme de protéine liée à la membrane et sa forme soluble est produite par un clivage protéolytique. Même si la désintégrine métalloprotéase ADAM17 est considérée comme la principale sheddase agissant sur le TNF-α, on ignore si ADAM17 est la seule responsable de ce processus pour tous les types de cellules. Afin d'identifier les sheddases de TNF-α dans une variété de cellules, nous avons réalisé des expériences à l'aide d'un système de criblage unique et nous avons observé que ADAM9, ADAM10, ADAM17 et ADAM19 sont capables de cliver le TNF-α. Nous avons ensuite réalisé des expériences d'interférence par ARN et nous avons confirmé que ADAM10 et ADAM17 sont effectivement impliquées dans la libération du TNF-α chez les cellules 293A. Chez les macrophages de souris, ADAM17 s'est avérée comme sheddase principale mais l'implication de ADAM10 a aussi été démontrée. Chez les cellules NIH3T3, ADAM10 pourrait être plus importante pour la libération que ADAM17. Dans la lignée cellulaire vasculaire endothéliale UV-2, ADAM10 et ADAM17 sont également impliquées dans la libération de TNF-α, alors que ADAM17 est la principale sheddase chez les chondrocytes ostéoarthritiques humains. À partir de ces observations et d'autres, nous avons conclu que ADAM10 et ADAM17 peuvent toutes deux être des sheddases du TNF-α et que leur importance pourrait être déterminée par leur niveau d'expression et par l'abondance des TIMP (« tissue inhibitor of metalloprotéinases »).

Mots-clés : TNF-α, ADAM10, ADAM17, TIMP, libération d'ectodomaine.

[Traduit par la Rédaction]

Introduction

Ectodomain shedding is a process in which transmembrane proteins are proteolytically released from the plasma membrane. Ectodomain shedding modifies the biologic and pathologic functions of the substrate protein. For example, amyloid precursor protein is cleaved by a disintegrin and metalloproteinase (ADAM) or the β-site of amyloid precursor protein cleaving enzyme and converted to a nonpathogenic and a pathogenic protein, respectively (Selkoe 1991; Buxbaum et al. 1998; Koike et al. 1999; Lammich et al. 1999; Vassar et al. 1999; Li et al. 2000). On the other hand, Fas ligand is cleaved by ADAM10 and largely loses its activity (Schneider et al. 1998; Schulte et al. 2007).

Tumor necrosis factor-α (TNF-α) is a pro-inflammatory cytokine that is involved in various pathologic conditions

Received 26 January 2009. Revision received 31 March 2009. Accepted 3 April 2009. Published on the NRC Research Press Web site at bcb.nrc.ca on .

A. Hikita, N. Tanaka, S. Yamane, Y. Ikeda, H. Furukawa, S. Tohma, R. Suzuki, H. Mitomi, and N. Fukui.[1] Department of Pathomechanisms, Clinical Research Center, National Hospital Organization Sagamihara Hospital, Sagamihara, Kanagawa 228-8522, Japan.

S. Tanaka. Department of Orthopaedic Surgery, Faculty of Medicine, University of Tokyo, Hongo 7-3-1, Tokyo, Japan.

[1]Corresponding author (e-mail: n-fukui@sagamihara-hosp.gr.jp).

doi:10.1139/O09-015

Published by NRC Research Press

such as rheumatoid arthritis, osteoarthritis, Crohn's disease, and endotoxin shock (Tracey et al. 1987; Kriegler et al. 1988; Brennan et al. 1989; Reinecker et al. 1993; Fernandes et al. 2002). TNF-α is expressed mainly by hematopoietic cells such as macrophages and T lymphocytes but is also present in nonhematopoietic cells such as mast cells and vascular endothelial cells (Carswell et al. 1975; Kobayashi et al. 1986; Steffen et al. 1989; Nilsen et al. 1998). In those cells, TNF-α is initially synthesized as a transmembrane protein and then becomes a soluble form via ectodomain shedding (McGeehan et al. 1994; Mohler et al. 1994).

Like other proteins, the pathologic significance of TNF-α may differ between membrane-bound and soluble forms. Soluble TNF-α is responsible for endotoxin shock because the blockade of TNF-α release protected mice from death (Mohler et al. 1994). On the other hand, TNF-α-deficient mice reconstituted with mutated TNF-α (muTNF delta 1–12), which lost its activity when cleaved into a soluble form, were shown to develop experimental hepatitis (Küsters et al. 1997). The role of TNF-α shedding in arthritis is controversial. The muTNF delta 1–12 mice developed arthritis spontaneously, implying that membrane-bound TNF-α may be important in its etiology (Alexopoulou et al. 1997). On the contrary, tissue inhibitor of metalloproteinase (TIMP)-3-deficient mice were more susceptible to bovine serum albumin induced arthritis (Mahmoodi et al. 2005). Since TNF-α shedding by ADAM17 was likely to be enhanced in those mice, that result might indicate the importance of soluble TNF-α in the development of arthritis.

Several proteinases are known to cleave TNF-α into a soluble form. At present, ADAM17 (also called TNF-α converting enzyme, or TACE) is thought to be the major sheddase for TNF-α (Black et al. 1997; Moss et al. 1997; Condon et al. 2001; Zheng et al. 2004; Bell et al. 2007; Horiuchi et al. 2007). In T lymphocytes, deficiency or suppression of ADAM17 blocked solubilization of membrane-bound TNF-α (Black et al. 1997; Condon et al. 2001). In mouse embryonic fibroblasts, deficiency of ADAM17 resulted in suppression of phorbol 12-myristate 13-acetate stimulated TNF-α shedding (Zheng et al. 2004). More recently, two other groups reported that ADAM17 is the primal sheddase for TNF-α in mouse macrophages (Bell et al. 2007; Horiuchi et al. 2007). However, these results do not necessarily mean that ADAM17 is the primal TNF-α sheddase in all types of cells because the endogenous sheddase for a substrate protein can differ from cell to cell. For example, the sheddase for receptor activator of NF-κb ligand (RANKL) in the mouse bone stromal cell line TM8B2 is mainly ADAM10, but a large part of soluble RANKL is produced by membrane type-1 matrix metalloproteinase (MT1-MMP) in osteoblasts (Hikita et al. 2006). Thus, the endogenous sheddase for TNF-α should be determined in the respective cell types.

In this study, we attempted to identify the endogenous TNF-α sheddase in several types of cells using a screening system for proteinases.

Materials and methods

Reagents

DNA polymerase, KOD plus, was purchased from TOYOBO (Osaka, Japan). Antibodies were obtained from the following companies: TNF-α, Cell Signaling Technology Inc. (Beverly, Massachusetts); ADAM10, Kamiya Biochemical (Seattle, Washington); ADAM17, Santa Cruz Biotechnology, Inc. (Santa Cruz, California); actin, Sigma-Aldrich Co. (St. Louis, Missouri); V5 tag, Invitrogen (Carlsbad, California). Lipopolysaccharide (LPS) was purchased from Wako Pure Chemical Industries, Ltd. (Osaka, Japan). Recombinant mouse TIMP-1 and TIMP-2 were purchased from Acris Antibodies GmbH (Hiddenhausen, Germany) and recombinant mouse TIMP-3 from R&D Systems (Minneapolis, Minnesota). Recombinant human TIMP-1 and TIMP-3 were obtained from Daiichi Fine Chemical (Toyama, Japan) and R&D Systems, respectively.

Cell culture

The human kidney cell line 293A (Invitrogen), mouse fibroblastic cell line NIH3T3, and mouse vascular endothelial cell line UV♀2 (RCB1994) (Riken BioResource Center, Tsukuba, Japan) were cultured in Dulbecco's modified Eagle medium (D-MEM) (Wako Pure Chemical Industries, Ltd.) supplemented with 10% FBS (SAFC Biosciences, Lenexa, Kansas) and 1% penicillin–streptomycin solution (Sigma-Aldrich Co.). Macrophages were collected from spleens of 4- to 6-week-old male ddy mice and cultured in α-MEM (Invitrogen) supplemented with 10% FBS, 1% penicillin–streptomycin solution, and 200 ng/mL M-CSF from the culture supernatant of CMG14-12 (a generous gift from Dr. Sunao Takeshita, Department of Bone and Joint Disease, Research Institute, National Center for Geriatrics and Gerontology, Obu City, Japan). Methods for collection and culture of human chondrocytes were previously described (Fukui et al. 2006). In brief, human articular chondrocytes were obtained from osteoarthritic knee cartilage at prosthetic surgery. The chondrocytes were isolated from the surrounding matrix by serial enzymic digestion and cultured in monolayer at the density of 2×10^5 cells/cm^2 in D-MEM/F-12 containing 10% FBS, 25 μg/mL ascorbic acid, and penicillin–streptomycin. Cells were incubated at 37 °C in a humidified atmosphere containing 5% CO_2. Expression vectors were transfected to these cells using FuGENE 6 transfection reagent (Roche Diagnostics, Indianapolis, Indiana) according to the manufacturer's instructions.

Constructs

cDNA of mouse TNF-α was cloned from cDNA of mouse macrophages by PCR and inserted in pCR-blunt II TOPO (Invitrogen) using protocols recommended by the manufacturer. The cDNA encoding TNF-α was subcloned into pSG5 vector (Stratagene, La Jolla, California) together with cDNA for myc or V5 and His tag subcloned from pCMV-Tag5A (Stratagene) or pcDNA3.1-V5HisA (Invitrogen), respectively. The (TNF-SEAP expression vector was constructed by inserting the cDNA fragment of the mouse TNF-α (corresponding to amino acids 1–90 including the cytoplasmic region, the transmembrane domain, and the stalk region) and the cDNA for SEAP subcloned from pSEAP2-Control (Clontech, Palo Alto, California) into pcDNA3.1-V5HisA. The construction of the expression vector for ADAM10 was previously described (Hikita et al. 2006). Expression vectors for ADAM9, ADAM17, ADAM19, and MMP7 were con-

structed by inserting the cDNA subcloned from corresponding pcDNA3.1-V5HisA constructs (Hikita et al. 2006) along with V5 and His tag into pSG5 vector. Expression vectors for MT1-MMP, MT2-MMP, MT3-MMP, MT4-MMP, MT5-MMP, and MT6-MMP were generous gifts from Dr. Motoharu Seiki (Center for Experimental Medicine, Institute of Medical Science, The University of Tokyo). Expression vectors for TIMP-1, TIMP-2, and TIMP-3 were constructed by inserting cDNA coding in these TIMPs to the *Eco*RI and *Xba*I sites of pcDNA3.1-V5HisA. Short hairpin RNA (shRNA) plasmids for GFP, mouse or human ADAM10 and ADAM17, and mouse TIMP-1 were constructed using piGENE mU6 vector or piGENE hU6 vector (iGENE Therapeutics Inc., Tsukuba, Japan) according to the manufacturer's protocol. Target sites are listed in Table 1. Retroviral shRNA vectors were constructed as follows: cDNA fragments for shRNA including the mouse U6 promoter were subcloned from piGENE constructs by PCR using M13F and M13R primers and ligated into pCR-blunt II TOPO (Invitrogen), digested by *Eco*RI, and inserted in the *Eco*RI site of pMX-IRES-bsr (a generous gift from Dr. Sunao Takeshita).

Screening of TNF-α sheddases

Alkaline phosphatase activity in culture media was assayed by a previously described method except for the use of tTNF-SEAP instead of tRANKL-SEAP (Hikita et al. 2005). The method for Western blot analysis was also described previously (Yamamoto et al. 2002). Soluble TNF-α in culture media was precipitated at 85% saturation of ammonium sulfate (Mueller et al. 1999), dissolved in TNE buffer [10 mmol/L Tris-HCl (pH 7.5), 150 mmol/L NaCl, 1 mmol/L EDTA, 1% NP-40], and subjected to SDS–PAGE. Soluble TNF-α was collected using Ni-NTA beads (Qiagen, Hilden, Germany) when it contained 6x His tag.

Determination of cleavage sites of TNF-α

pSG5-mTNFα-V5His was transfected to 293A cells. Seventy-two hours after transfection, 200 mL of culture medium was collected and soluble TNF-α was recovered using Ni-NTA beads. Samples were subjected to SDS–PAGE, transferred to polyvinylidene membrane, and stained with Coomassie Brilliant Blue. The band was excised and the N-terminal amino acid sequence was determined by Hokkaido System Science Co., Ltd. (Hokkaido, Japan).

ELISA

The concentration of soluble TNF-α in culture media was determined using a Murine TNF-α ELISA development kit (Peprotech, Rocky Hill, New Jersey) for mouse macrophages and NIH3T3 and UV‡2 cells. The amount of TNF-α released from primary cultured chondrocytes was determined as follows. Forty-eight hours after plating, culture media were replaced with those containing 3 μg/mL LPS. For some cells, recombinant human TIMP-1 or TIMP-3 was added to the media at a concentration of 100 nmol/L. Twenty-four hours later, the media were collected and the amount of TNF-α was determined by ELISA (QuantiGlo Chemiluminescent Sandwich ELISA kit, R&D Systems).

Table 1. Target sequences for RNAi.

Gene	Sequence
GFP	5′-GCTACGTCCAGGAGCGCACCA-3′
Mouse *Adam10*	5′-GACATTATGAAGGATTATCTT-3′
	5′-GGGTCTGTCATTGATGGAAGA-3′
Mouse *Adam17*	5′-GCGACACACTTAGAAACATTA-3′
	5′-GGAACTCTTGGATTAGCTTAC-3′
Human *ADAM10*	5′-GACATTATGAAGGATTATCTT-3′
	5′-GGTCTCATGTACCTCCCAAAG-3′
Human *ADAM17*	5′-GCTCTCAGACTACGATATTCT-3′
	5′-GCTAGAGCAATTTAGCTTTGA-3′
Mouse *Timp1*	5′-GCAACTCGGACCTGGTCATAA-3′
	5′-GGAACGGAAATTTGCACATCA-3′
	5′-GCACAGTGTTTCCCTGTTTAT-3′

Note: GFP was used as a control.

Real-time RT-PCR

The reaction mixture for real-time RT-PCR was prepared using SYBR Premix Ex *Taq* (TAKARA Biochemicals, Shiga, Japan) and analyzed using LightCycler (Roche Applied Science, Indianapolis, Indiana) according to the manufacturer's protocol. The sets of primers used are listed in Table 2.

Retrovirus infection

The procedure for the preparation of the retrovirus was described previously (Kitamura 1998). Spleen macrophages were incubated with culture media containing retrovirus supplemented with 4 μg/mL polybrane (Sigma-Aldrich Co.) and 200 ng/mL M-CSF for 6 h. Eighteen hours later, infected cells were selected by culturing in the media containing 1 μg/mL blasticidin S (Kaken Pharmaceutical Co., Tokyo, Japan) for 48 h.

Immunostaining

A skin biopsy specimen was obtained from a 57-year-old female patient with Henoch-Schönlein purpura, and a control specimen was acquired from a 73-year-old female who died of an unrelated cause. Immunostaining of the skin tissues was performed as follows. Four-micrometre-thick sections were prepared, deparaffinized in xylene, and rehydrated in graded concentrations of ethanol. After blocking endogenous peroxidase activity, antigen retrieval was performed by autoclaving sections for 30 min in Target Retrieval Solution (pH 6.0) (Dako Japan, Tokyo, Japan). Primary antibodies for ADAM10 and TNF-α were both purchased from Abcam (Cambridge, Masschusetts) and used at a concentration of 1/100. Color detection of those antibodies was performed by a commercially available kit (EnVision HRP kit, Dako Japan). Immunostaining of cartilage tissue was described before (Fukui et al. 2006). In brief, 6-μm-thick cryosections were prepared from osteoarthritic or control cartilage, fixed with ice-cold acetone, and digested with sheep testis hyaluronidase (type IV, Sigma-Aldrich Co.) for antigen retrieval. Osteoarthric cartilage was obtained at prosthetic surgery, and control cartilage was obtained from a nonarthritic knee joint of a donor who died of an unrelated disease. The anti-ADAM10 and anti-TNF-α antibodies were used at a concentration of 1:100 and visualized with a commercially available kit (ABC Staining System, Santa Cruz Biotechnology)

Table 2. Primer sequences for mouse genes and human genes used for real-time PCR.

Gene	Forward	Reverse
Mouse		
Adam9	5′-GGATATGGAGGAAGCGTGGA-3′	5′-GCAACAAGGGGGACGATTAG-3′
Adam10	5′-AGCAACATCTGGGGACAAAC-3′	5′-TGGCCAGATTCAACAAAACA-3′
Adam17	5′-GTACGTCGATGCAGAGCAAA-3′	5′-GAAATCCCAAAATCGCTCAA-3′
Adam19	5′-GGTTCTGCTTGCTGGCTCTC-3′	5′-CCTTCTTGGCTTCCTCTTGTG-3′
Mmp7	5′-AGGCGGAGATGCTCACTTTG-3′	5′-GGTGGCAGCAAACAGGAAG-3′
Mmp14 (MT1-MMP)	5′-CCCAAGGCAGCAACTTCA-3′	5′-CAATGGCAGCTGAGAGTGAC-3′
Mmp16 (MT3-MMP)	5′-ATCATGGCCCCATTTTATCA-3′	5′-GCATTGGGTATCCATCCATC-3′
Mmp24 (MT5-MMP)	5′-TTGAGCAGGAGGAGGAGAAA-3′	5′-GAGTCACCTTCTGCCACACA-3′
Timp1	5′-ATCTGGCATCCTCTTGTTGC-3′	5′-CGTTGATTTCTGGGGAACC-3′
Timp2	5′-CACCCAGAAGAAGAGCCTGA-3′	5′-GTGACCCAGTCCATCCAGAG-3′
Timp3	5′-GCGTGTATGAAGGCAAGATGTA-3′	5′-GAGGTCACAAAACAAGGCAAGTA-3′
Actb (actin, beta)	5′-AGATGTGGATCAGCAAGCAG-3′	5′-GCGCAAGTTAGGTTTTGTCA-3′
Freyer et al. (1999)		
ADAM10	5′-TTTGAAGGATTCATCCAGACTC-3′	5′-ACACCAGTCATCTGGTATTTCC-3′
ADAM17	5′-AAGCTTGATTCTTTGCTCTCAG-3′	5′-TACTCGCTTTCGTTTTTACCAT-3′
TIMP1	5′-AGCGTTATGAGATCAAGATGACCA-3′	5′-GTTTTCCAGCAATGAGAAACTCCT-3′
TIMP2	5′-ATGATAGGTGAACCTGAGTTGCAG-3′	5′-CTATCCTAACCCCCATATCACTGG-3′
TIMP3	5′-AACTCCGACATCGTGATCCG-3′	5′-CGTAGTGTTTGGACTGGTAGC-3′
GAPDH	5′-AAAACCTGCCAAATATGATGAC-3′	5′-CAGGAAATGAGCTTGACAAAGT-3′

coupled with 3-amino-9-ethylcarbazole (AEC Liquid Substrate Chromogen, Dako Japan).

Results

Screening of MMPs and ADAMs as TNF-α sheddases

We constructed an expression vector encoding a fusion protein of secreted placental alkaline phosphatase (SEAP) with the C-terminally truncated form of TNF-α, which contained the stalk region, the transmembrane domain, and the intracellular domain of TNF-α (tTNF-SEAP) (Fig. 1A). Expression vectors of various MMPs or ADAMs were transfected to 293A cells together with tTNF-SEAP plasmids and the alkaline phosphatase activity of culture media was measured. To achieve sufficient levels of proteinase expression, proteinase expression vectors were transfected in 80-fold excess of the tTNF-SEAP expression vector. In this assay system, increased alkaline phosphatase activity in the medium indicates an increase in TNF-α shedding. ADAM9, ADAM10, ADAM17, ADAM19, MMP7, MT1-MMP, MT3-MMP, and MT5-MMP exhibited tTNF-SEAP shedding activities (Fig. 1B). In contrast, MMP1, MMP2, MMP3, MMP9, MMP11, MMP13, MMP23, MMP28, MT2-MMP, MT4-MMP, and MT6-MMP failed to cleave tTNF-SEAP (data not shown).

ADAM10 and ADAM17 are major TNF-α sheddases in 293A cells

To confirm the capacity of these proteinases to cleave full-length TNF-α, they were expressed in 293A cells together with full-length TNF-α, which was C-terminally tagged with myc. In this experiment, expression vectors for proteinases and those for TNF-α were transfected at an equal molarity. Soluble TNF-α was recovered from culture media by ammonium sulfate precipitation and subjected to Western blotting analysis. When TNF-α was overexpressed

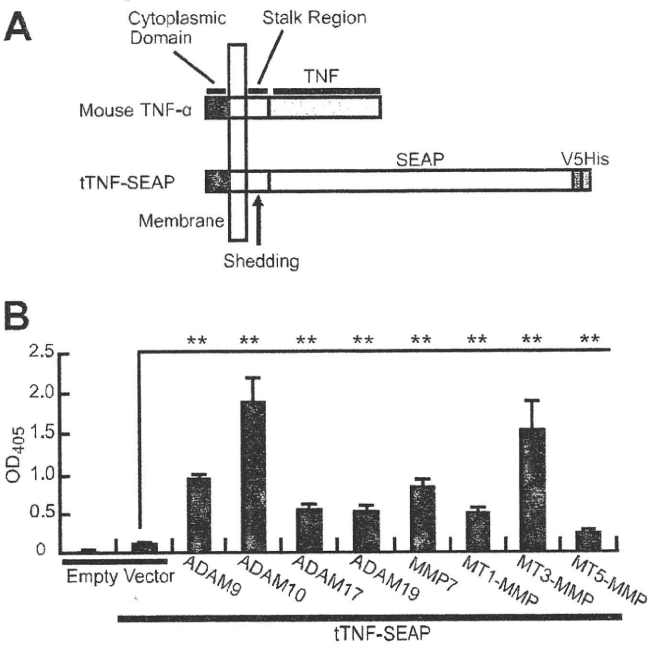

Fig. 1. Screening of potential TNF-α sheddases. MMPs, and ADAMs. (A) Schematic representations of TNF-α and the tTNF-SEAP fusion protein. tTNF-SEAP is a fusion protein of SEAP with C-terminally truncated TNF-α, which contains the stalk region but lacks the TNF domain. The protein has a V5 and 6x His tag at the C terminus. Cleavage of tTNF-SEAP can be evaluated by alkaline phosphatase activity in culture supernatants. (B) Alkaline phosphatase activity of culture media of 293A cells transfected with tTNF-SEAP and expression vectors for ADAMs or MMPs. $^{**}P < 0.01$.

in 293A cells, soluble TNF-α cleaved by endogenous proteinase in the cells appeared in culture media (Fig. 2A). The N-terminal sequence of soluble TNF-α was determined (Fig. 2B), which agreed with the cleavage site reported pre-

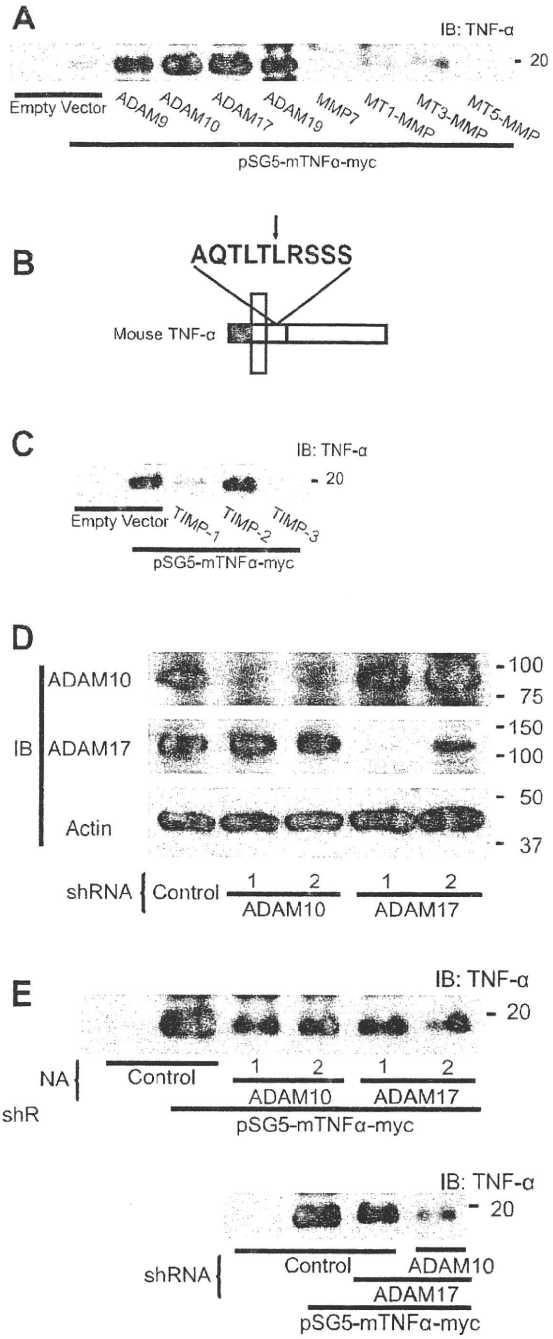

Fig. 2. Shedding of TNF-α in 293A cells. (A) Shedding of full-length TNF-α. 293A cells were transfected with pSG5-mTNFα-myc together with plasmids expressing MMPs or ADAMs. Seventy-two hours later, culture media were collected and proteins were precipitated with ammonium sulfate and subjected to Western blotting analysis using anti-TNF-α antibody. Soluble TNF-α was detected as a band of approximately 20 kDa. (B) Cleavage site of TNF-α in 293A cells. (C) Inhibition of TNF-α shedding by endogenous proteinases with TIMPs. 293A cells were transfected with pSG5-mTNFα-myc and pcDNA3.1-TIMP1-V5HisA, pcDNA3.1-TIMP2-V5HisA, or pcDNA3.1-TIMP3-V5HisA. Shedding of TNF-α was determined as described for Fig. 2A. (D) Suppression of ADAM10 and ADAM17 by RNAi. shRNA plasmids for ADAM10 or ADAM17 were transfected to 293A cells, and 48 h later, cell lysates were obtained and subjected to Western blotting analysis to evaluate suppression of endogenous ADAM10 or ADAM17. (E) Effects of RNAi for ADAM10 and ADAM17 on the shedding of TNF-α. 293A cells were transfected with pSG5-mTNFα-myc and shRNA plasmids for ADAM10 or ADAM17. Shedding of TNF-α was evaluated in the same manner.

viously (Cseh and Beutler 1989). Among proteinases that had cleaved tTNF-SEAP, ADAM9, ADAM10, ADAM17, and ADAM19 showed shedding activities for full-length TNF-α (Fig. 2A). The cleavage of TNF-α by MMP7, MT1-MMP, MT3-MMP, and MT5-MMP was relatively low compared with the result of the screening using tTNF-SEAP (Fig. 1B). TIMPs are biologic inhibitors for metalloproteinases and four subtypes have been reported (Gomez et al. 1997). Spectra of inhibition are different among the subtypes, so TIMPs have been widely used for identification of endogenous proteinase(s). To identify the endogenous sheddase(s) in 293A cells, expression vectors for TIMP-1, TIMP-2, and TIMP-3 were cotransfected with an expression vector for full-length TNF-α to 293A cells. Overexpression of TIMP-1 and TIMP-3 decreased soluble TNF-α in culture media, while TIMP-2 had no apparent effect (Fig. 2C). This result ruled out the involvement of ADAM9 or ADAM19 in TNF-α shedding because the activities of these proteinases are not inhibited by any of those three TIMPs (Amour et al. 2002; Chesneau et al. 2003). Meanwhile, the reduction of soluble TNF-α by TIMP-1 and TIMP-3 suggested the involvement of ADAM10 in the shedding, since the activity of ADAM10 is inhibited by these TIMPs (Amour et al. 2000). The involvement of ADAM17 was also possible because ADAM17 is inhibited by TIMP-3 (Amour et al. 1998).

To clarify the involvement of these two ADAMs, shRNA vectors for ADAM10 and ADAM17 were constructed. Transfection of these constructs specifically reduced the expression of ADAM10 and ADAM17, respectively (Fig. 2D). Suppression of ADAM10 or ADAM17 resulted in decrease of soluble TNF-α in the culture media, and a further reduction was observed by simultaneous suppression of these two ADAMs (Fig. 2E). These results indicated that ADAM10 and ADAM17 are two major TNF-α sheddases in 293A cells.

Determination of endogenous sheddase(s) for TNF-α in macrophages

Macrophages are known to express several ADAMs (Verrier et al. 2004). To confirm the expression of proteinases that had shedding activities for tTNF-SEAP, RNA from macrophages with or without LPS treatment was analyzed by real-time RT-PCR. Considerable amounts of ADAM9, ADAM10, ADAM17, and MT1-MMP were expressed in macrophages with or without LPS stimuli, but the expression of ADAM19, which showed a shedding activity for full-length TNF-α, was considerably lower than that of the other four proteinases (Fig. 3A). Because ADAM10, one of the major TNF-α sheddases in 293A cells, is expressed in macrophages at a level comparable with ADAM17, we attempted to specify the endogenous sheddase(s) for TNF-α in macrophages. LPS was able to stimulate macrophages to release soluble TNF-α to culture media (Carswell et al. 1975). To identify the endogenous TNF-α sheddase(s), re-

Fig. 3. Shedding of TNF-α in mouse spleen macrophages. (A) Expression of MMPs and ADAMs in mouse spleen macrophages. After culturing for 16 h in the presence or absence of LPS (1 μg/mL). RNA was obtained and the expression of respective genes was analyzed by real-time RT-PCR together with that of β-actin. Results are shown by expression ratios against β-actin. (B) Inhibition of TNF-α shedding by TIMPs. Macrophages were cultured with or without 1 μg/mL LPS for 16 h together with recombinant TIMPs at the indicated concentrations and the concentration of soluble TNF-α in culture media was measured by ELISA. $*P < 0.05$; $**P < 0.01$. (C) RNAi for ADAM10 and ADAM17. Macrophages were infected with retroviruses containing shRNA sequence and infected cells were selected with 1 μg/mL blasticidin S for 48 h. RNA was extracted from cells and gene expression was analyzed by real-time RT-PCR. $**P < 0.01$. (D) Effects of RNAi for ADAM10 and ADAM17 on the shedding of TNF-α. Retroviruses containing shRNA sequence for ADAM10 or ADAM17 were infected to macrophages and infected cells were selected with 1 μg/mL blasticidin S for 48 h. Some cells were then treated with 1 μg/mL LPS. Sixteen hours later, soluble TNF-α in culture media was measured by ELISA. $**P < 0.01$.

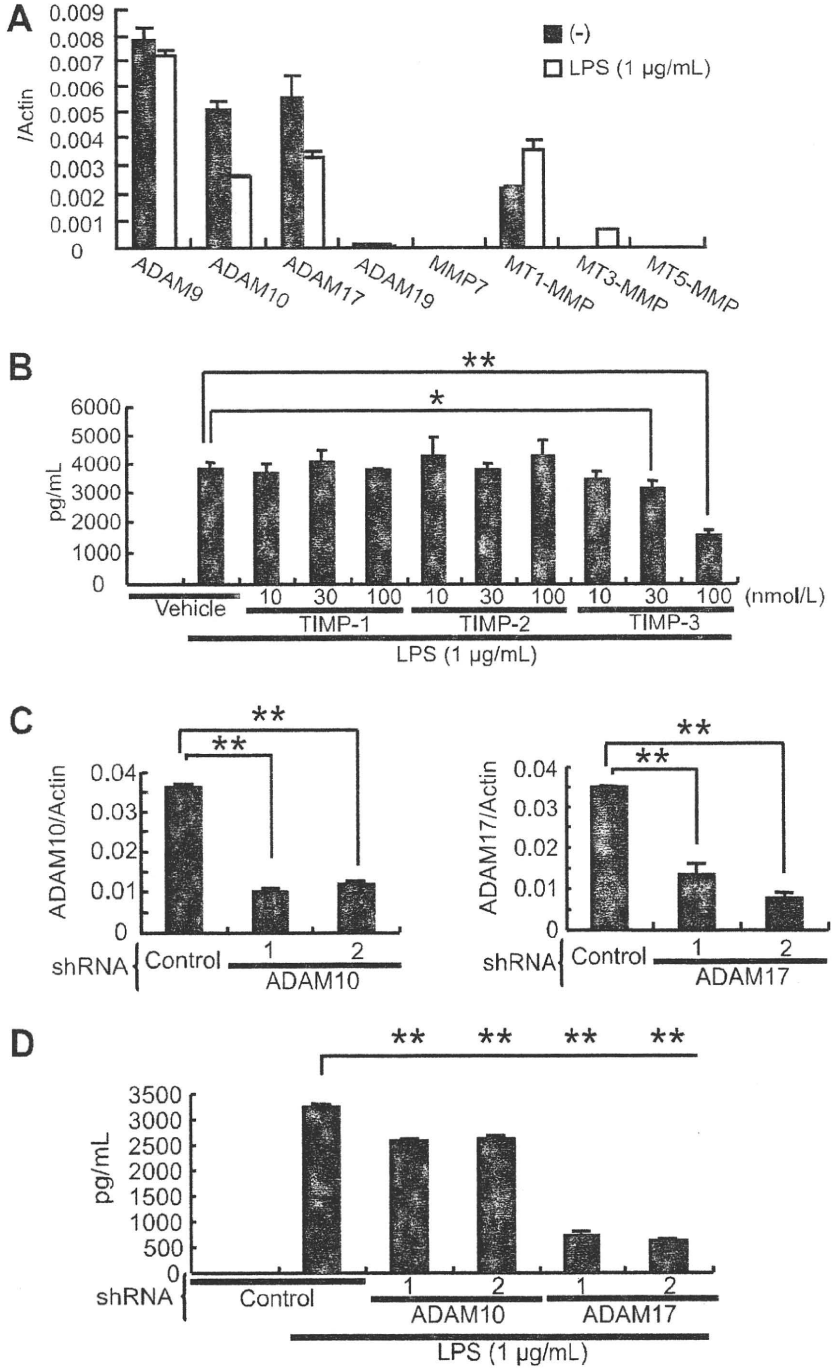

combinant TIMP-1, TIMP-2, and TIMP-3 were added to culture media together with LPS and the concentration of soluble TNF-α in culture media was determined by ELISA. TIMP-3 suppressed shedding of TNF-α in a dose-dependent manner, while TIMP-1 and TIMP-2 failed to suppress it (Fig. 3B). This result suggested that ADAM17 might be the

endogenous sheddase in macrophages, while ADAM10 could have little contribution to the shedding. To confirm this, we constructed retroviral vectors carrying shRNA for these proteinases. Suppression of ADAM10 or ADAM17 expression by those retrovirus vectors was confirmed by real-time RT-PCR (Fig. 3C). Using these vectors, the involvement of these two proteinases in TNF-α shedding was investigated in macrophages. RNAi for ADAM17 dramatically suppressed TNF-α shedding with LPS stimulation (Fig. 3D). On the other hand, suppression of ADAM10 showed a partial effect on the concentration of soluble TNF-α with LPS stimuli. These results confirmed the results of previous studies that ADAM17 is the major sheddase in macrophages (Bell et al. 2007; Horiuchi et al. 2007).

TIMP-1 inhibits ADAM10 activity in macrophages

Although ADAM10 played a significant role in TNF-α shedding in 293A cells, it was not a major TNF-α sheddase in macrophages in spite of its substantial expression. In an attempt to understand this seeming contradiction, we evaluated expression levels of ADAM10, ADAM17, TIMP-1, TIMP-2, and TIMP-3 in macrophages. In macrophages, ADAM10 was expressed at a level similar to that of ADAM17 (Fig. 3A). Meanwhile, TIMP-1 may be expressed more abundantly than TIMP-3, and that trend was augmented when the cells were stimulated with LPS (Fig. 4A). Considering the difference in inhibitory effects between these TIMPs, such a difference in their expression may account for the major role of ADAM17 in TNF-α shedding in macrophages. To confirm this speculation, we made retroviruses carrying shRNAs for TIMP-1 and evaluated their effects on the release of TNF-α (Fig. 4B). Suppression of TIMP-1 in macrophages by these constructs in fact increased shedding of TNF-α (Fig. 4C). Thus, the activity of ADAM10 was considered to be suppressed in macrophages by the abundance of endogenous TIMP-1.

ADAM10 is the major TNF-α sheddase in NIH3T3 cells

The endogenous sheddase(s) for a substrate protein may differ from cell to cell. As shown above, the endogenous sheddase(s) could be determined by the expression of the proteinase(s) and its endogenous inhibitor(s). Thus, we next examined expression of ADAM10, ADAM17, TIMP-1, TIMP-2, and TIMP-3 in NIH3T3. Compared with macrophages, NIH3T3 cells expressed ADAM10 more abundantly than ADAM17 (Fig. 5A). In NIH3T3, the difference in expression between TIMP-1 and TIMP-3 was not so obvious as in macrophages (Fig. 5B). These data suggested that ADAM10 could have a greater contribution to TNF-α shedding in NIH3T3 than in macrophages. shRNA vectors for mouse ADAM10 and ADAM17 showed specific inhibition of respective proteinases in this cell line (Fig. 5C). These constructs were transfected with an expression vector for full-length TNF-α, and soluble TNF-α was collected from culture media using Ni-NTA beads. Although suppression of ADAM10 or ADAM17 resulted in reduction of soluble TNF-α, the reduction was more obvious with the suppression of ADAM10 than with that of ADAM17 (Figs. 5D and 5E). This result indicated that unlike in macrophages, ADAM10 is the major TNF-α sheddase in NIH3T3 cells.

Fig. 4. Suppression of TNF-α shedding by TIMP-1 in mouse spleen macrophages. (A) Expression of TIMPs in mouse spleen macrophages. Expression of TIMP-1, TIMP-2, and TIMP-3 in macrophages was determined by real-time RT-PCR as described for Fig. 3A. Results are shown by expression ratios against β-actin. (B) RNAi for TIMP-1. Effect of retroviruses carrying shRNA constructs for TIMP-1 was confirmed in the manner described for Fig. 3D. Expression of TIMP-1 is shown by the ratios against that of β-actin. (C) Effects of RNAi for TIMP-1 on the shedding of TNF-α. TIMP-1 expression was suppressed and the change of TNF-α release into the media was evaluated as described for Fig. 3D.

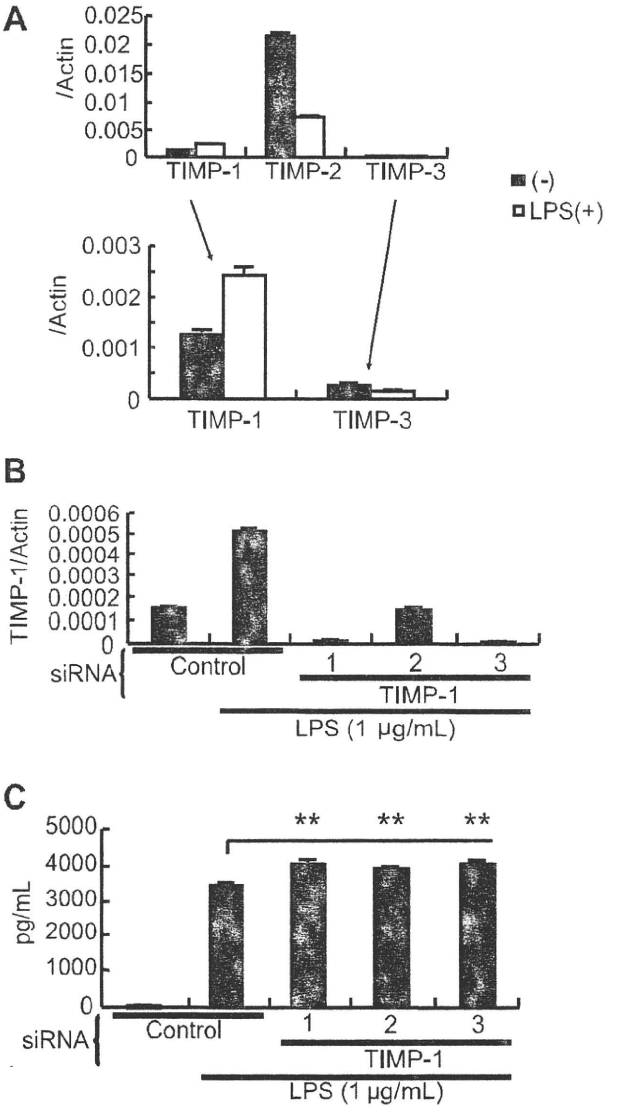

Involvement of ADAM10 and ADAM17 in TNF-α shedding in vascular endothelial cell line

Vascular endothelial cells were known to release TNF-α with several stimulations such as high-mobility group protein-1, cell walls of *Streptococcus pneumoniae*, and LPS. Such release of TNF-α by endothelial cells is profoundly involved in several pathologies such as sepsis or bacterial meningitis (Freyer et al. 1999; Fiuza et al. 2003). To identify the endogenous sheddase(s) for TNF-α in vascular endothelial cells, we conducted experiments using a mouse vascular endothelial cell line, UV♀2. In this cell, both

Fig. 5. Shedding of TNF-α in NIH3T3 cells. (A and B) Expression of ADAMs and TIMPs in NIH3T3 cells. RNA was obtained from NIH3T3 and expression of ADAM10 and ADAM17 (Fig. 5A) and TIMP-1, TIMP-2, and TIMP-3 (Fig. 5B) was analyzed by real-time RT-PCR. Results are shown by ratios against β-actin expression. (C) RNAi for ADAM10 and ADAM17. pSG5-ADAM10-V5HisA or pSG5-ADAM17-V5HisA was transfected to NIH3T3 cells together with shRNA plasmids for the gene. Cell lysate was obtained 48 h after transfection and subjected to Western blotting analysis. (D and E) Effects of RNAi for ADAM10 or ADAM17 on the shedding of TNF-α. NIH3T3 cells were transfected with pSG5-TNF-α-V5HisA and shRNA plasmids for ADAM10 or ADAM17. Seventy-two hours later, soluble TNF-α in culture media was collected using Ni-NTA agarose and subjected to Western blotting analysis (Fig. 5D) or measured directly by ELISA (Fig. 5E). $*P < 0.05$; $**P < 0.01$.

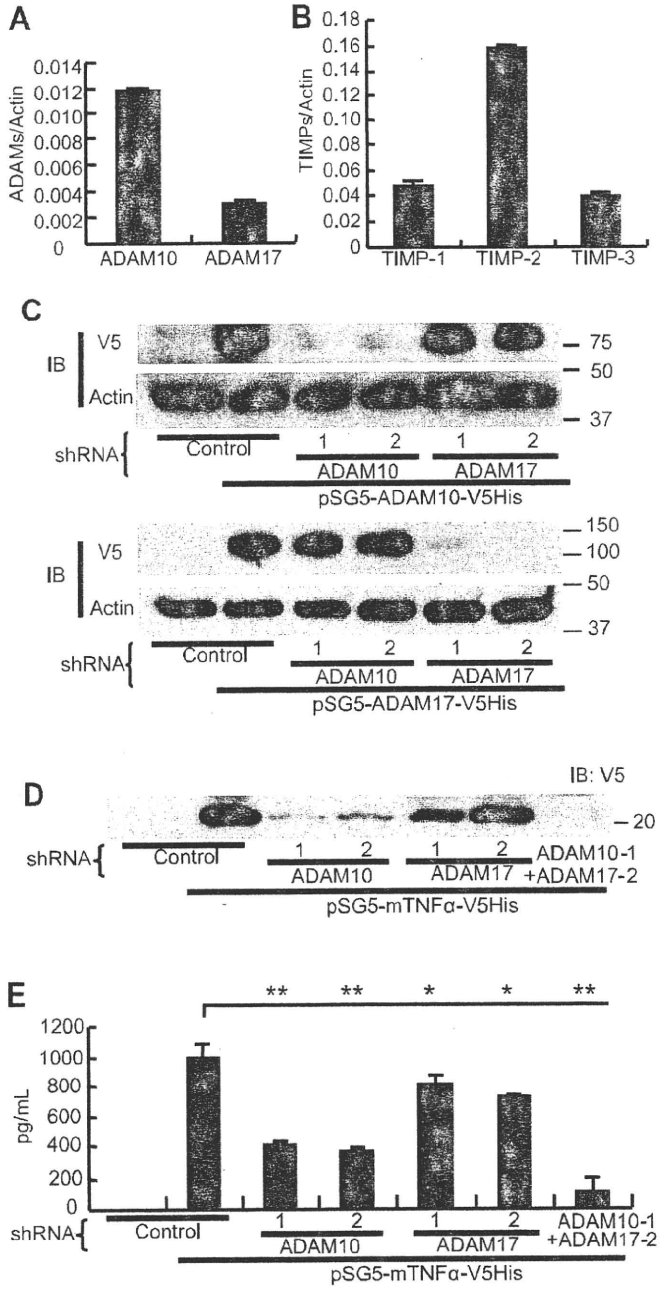

ADAM10 and ADAM17 were expressed at substantial levels with the preponderance of ADAM10, similar to that in NIH3T3 (Fig. 6A). Meanwhile, the pattern of expression between TIMP-1 and TIMP-3 differed from that of NIH3T3 but resembled that of macrophages in that the expression of TIMP-1 was higher than that of TIMP-3 (Fig. 6B). Overexpression of TNF-α in UV♀2 resulted in release of soluble TNF-α into culture media (Fig. 6C). shRNA vectors for ADAM10 and ADAM17 suppressed TNF-α shedding, respectively, and transfection of both vectors showed an additive effect (Figs. 6C and 6D). Thus, it was considered that both ADAM10 and ADAM17 are endogenous sheddases for TNF-α in vascular endothelial cells. We next investigated the involvement of ADAM10 in the pathology of human vasculitis. In the acute phase of Henoch-Schönlein purpura, a form of allergic vasculitis, the serum TNF-α level is known to increase, and endothelial cells are assumed to be the source of TNF-α (Besbas et al. 1997; Ha 2005). In a small vessel of Henoch-Schönlein purpura, positive stain for ADAM10 and TNF-α was seen not only in infiltrated leukocytes but also along the endothelium of the vessel, suggesting that TNF-α could be released by ADAM10 in this pathology (Figs. 6E–6H).

TNF-α sheddase in osteoarthritic chondrocytes

TNF-α also plays an important role in the pathology of osteoarthritis (Fernandes et al. 2002). In osteoarthritis, chondrocytes secrete TNF-α, which induces catabolism in chondrocytes in an autocrine manner (Pelletier et al. 2001). In accordance with previous reports, immunostaining of osteoarthritic cartilage confirmed that osteoarthritic chondrocytes were expressing TNF-α (Fig. 7A), while it was little expressed in control cartilage (Fig. 7B). Osteoarthritic chondrocytes were intensely stained for ADAM10, which indicated a possibility that ADAM10 could be involved in TNF-α shedding in those chondrocytes (Fig. 7C). Interestingly, chondrocytes in control cartilage were also positive for ADAM10, although the staining tended to be weaker (Fig. 7D). We then evaluated the expression of ADAM10, ADAM17, TIMP-1, TIMP-2, and TIMP-3 in the chondrocytes within osteoarthritic cartilage. Similar to NIH3T3 and UV♀2 cells, ADAM10 and ADAM17 were expressed at comparable levels in those cells (Fig. 7E). Meanwhile, the expression of TIMP-1 could be more abundant than that of TIMP-3, showing a possibility that the enzymatic activity of ADAM10 might be more suppressed in the cells than that of ADAM17 (Fig. 7F). To investigate the significance of ADAM10 and ADAM17 in TNF shedding, we conducted experiments using cultured chondrocytes. Chondrocytes obtained from osteoarthritic cartilage secreted a small amount of TNF-α (1×10^6 cells released approximately 10 pg of TNF-α in 24 h). Stimulation with LPS increased the amount of released TNF-α three- to ninefold. This release of TNF-α was strongly inhibited by TIMP-3, but a significant reduction was also observed with TIMP-1 (Fig. 7G). These results indicate that ADAM17 could be the major endogenous sheddase for TNF-α in osteoarthritic chondrocytes. Although expressed at a comparable level, the activity of ADAM10 might be inhibited largely by endogenous TIMP-1 abundantly expressed in the cells.

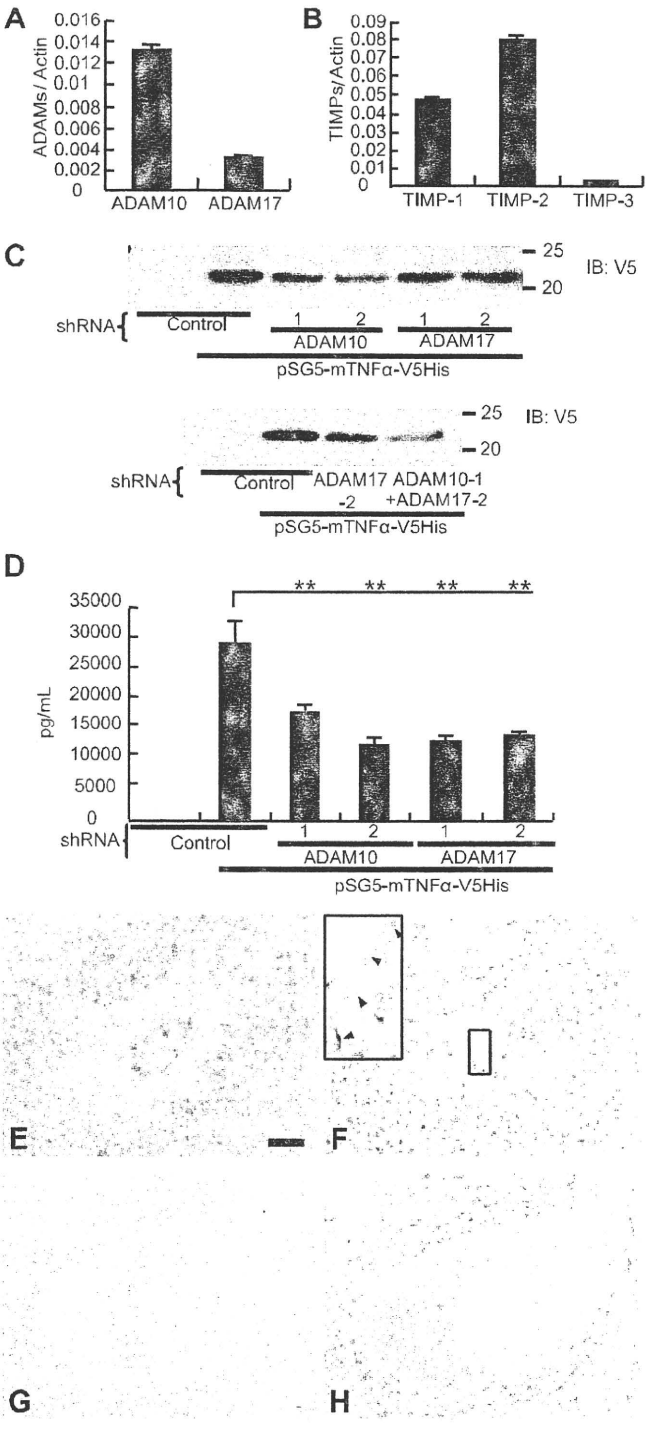

Fig. 6. Shedding of TNF-α in UV♀2 cells. (A and B) Expression of ADAMs and TIMPs in UV♀2 cells. RNA was obtained from UV♀2 cells and expression of ADAM10 and ADAM17 (Fig. 6A) and TIMP-1, TIMP-2, and TIMP-3 (Fig. 6B) was analyzed by real-time RT-PCR. Results are shown by ratios against β-actin expression. (C and D) Effects of RNAi for ADAM10 or ADAM17 on the shedding of TNF-α. UV♀2 cells were transfected with pSG5-mTNFα-V5His and shRNA plasmids for ADAM10 or ADAM17. Forty-eight hours later, soluble TNF-α in culture media was collected using Ni-NTA agarose and subjected to Western blotting analysis (Fig. 6C) or measured directly by ELISA (Fig. 6D). $^{**}P < 0.01$. (E–H) Expression of ADAM10 and TNF-α in vasculitic endothelium. Skin biopsy specimens obtained from a patient with Henoch-Schönlein purpura (Figs. 6E and 6F) and a control donor (Figs. 6G and 6H) were immunostained for ADAM10 (Figs. 6E and 6G) and TNF-α (Figs. 6F and 6H), respectively. In Fig. 6F, a higher magnification image of the boxed area is shown in the inset in which staining for TNF-α is indicated by arrowheads. Cross-sectional images of a blood vessel are shown. Bar = 50 μm.

Discussion

In this study, we employed a unique screening system to find possible sheddases for TNF-α. Although the system is not the one well established, we have already used a similar system to identify RANKL sheddases and found it to be a reliable method (Hikita et al. 2006). In this system, the result could be affected by expression levels of the proteinases. If proteinases are expressed at low levels, their capacity to cleave the substrate may be underestimated. To avoid this, in the present study, we transfected proteinase expression vectors in excessive amounts. Although there was some discrepancy between the result of the initial screening (Fig. 1B) and that of the second experiment with full-length TNF-α (Fig. 2A), it could not be related to the poor reliability of the screening but more likely to the difference in substrate proteins.

Currently, ADAM17 is considered to be the major sheddase for TNF-α (Black et al. 1997; Moss et al. 1997; Condon et al. 2001; Zheng et al. 2004; Bell et al. 2007; Horiuchi et al. 2007). However, besides ADAM17, several proteinases are known to cleave membrane-bound TNF-α. Haro et al. (2000) showed that MMP7 null macrophages failed to release soluble TNF-α, suggesting that MMP7 could be responsible for TNF-α shedding in macrophages. Purified proteinase 3 from activated neutrophils was also shown to have a shedding activity for TNF-α (Coeshott et al. 1999). ADAM19 could work as a sheddase for TNF-α when overexpressed in COS-7 and CHO cells (Chesneau et al. 2003). ADAM10 is also reported to have a shedding activity for TNF-α. Purified bovine ADAM10 and ADAM10 overexpressed in 293A EBNA cells processed TNF-α in vitro (Lunn et al. 1997). In contrast, when expressed in COS-7 cells or CHO cells, ADAM10 failed to release TNF-α (Zheng et al. 2004). Again, the lack of ADAM10 expression did not change TNF-α shedding in mouse embryonic fibroblasts (Zheng et al. 2004). In this study, we showed that not only ADAM17 but also ADAM9, ADAM10, and ADAM19 are capable of cleaving TNF-α in a cell-based assay. We also showed, for the first time, that endogenous ADAM10 is a major TNF-α sheddase in 293A cells, NIH3T3 cells, and UV♀2 cells. Our current result differed from those in previous reports in that endogenous ADAM10 can cleave TNF-α in certain types of cells. Since proteinases involved in protein shedding often differ among cell types (Schlöndorff et al. 2001; Hikita et al. 2006), the discrepancy between our current result and those reported previously could be ascribed to the difference in cell types used in the assay. Also, the difference in used constructs or substrate proteins could account for the discrepancy. In the report of Zheng et al. (2004), the expression vector for a fusion protein of alkaline phosphatase and TNF-α was used, while myc-tagged

Fig. 7. Shedding of TNF-α in articular chondrocytes. (A–D) Expression of TNF-α and ADAM10 in osteoarthritic and control cartilage. Histological sections of osteoarthritic and control cartilage were immunostained for TNF-α (Figs. 7A and 7B, respectively) and ADAM10 (Figs. 7C and 7D, respectively). Bar = 100 μm. (E and F) Expression of ADAMs and TIMPs in chondrocytes. RNA was obtained from human osteoarthritic chondrocytes and expression of ADAM10 and ADAM17 (Fig. 7E) and TIMP-1, TIMP-2 and TIMP-3 (Fig. 7F) was analyzed by real-time RT-PCR. Results are shown by ratios against GAPDH expression. (G) Effects of TIMP-1 and TIMP-3 on the secretion of TNF-α from primary cultured chondrocytes stimulated with LPS. $*P < 0.05$; $**P < 0.01$.

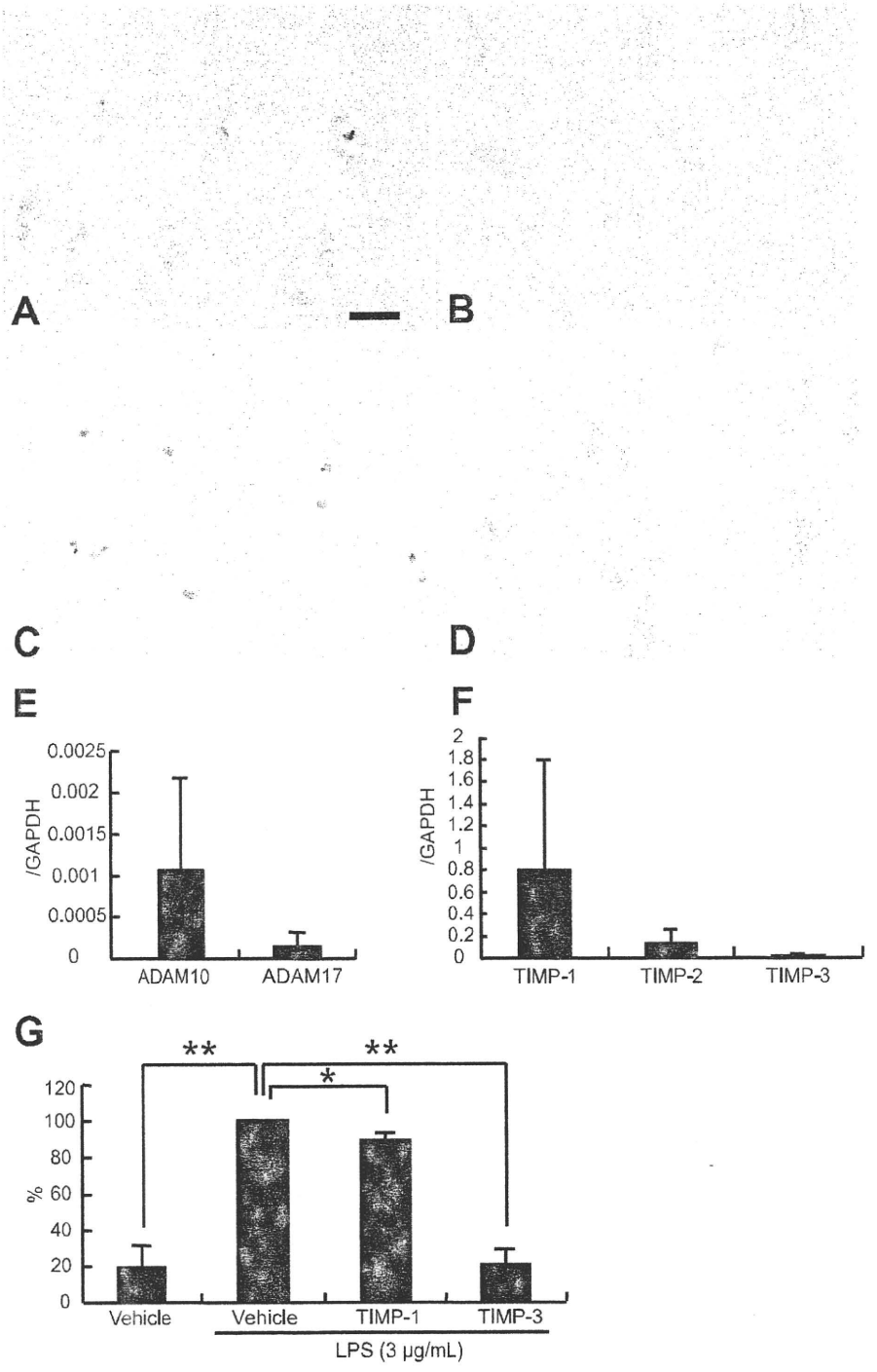

TNF-α was used in our assay. We often failed to detect alkaline phosphatase activity in the culture media of 293 cells when fusion proteins of the alkaline phosphatase and substrate proteins were overexpressed, possibly due to the interaction between the enzyme and the substrate proteins.

In this study, we confirmed that the major sheddase for TNF-α in macrophages is ADAM17. This result is consistent with those of two recent reports that dealt with ADAM17 conditional knockout mice and radiation chimeric mice reconstituted with leukocytes lacking functional ADAM17 (Bell et al. 2007; Horiuchi et al. 2007). ADAM10, which turned out to be the major TNF-α sheddase in the above-

mentioned three types of cells, was known to play only a limited role in the release of TNF-α in macrophages. This discrepancy could be explained by the difference in expression levels between ADAM10 and ADAM17. Compared with macrophages, the expression of ADAM10 was more abundant than that of ADAM17 in NIH3T3 cells. Likewise, in UV♀2 cells in which both ADAM10 and ADAM17 play significant roles in TNF-α shedding, the expression of ADAM10 was relatively greater than that of ADAM17. Presence of TIMPs may be another factor that determines the significance of the proteinases in the shedding. While the enzymic activity of ADAM10 was inhibited by TIMP-1 and TIMP-3, the activity of ADAM17 was suppressed by TIMP-3 but not by TIMP-1. In macrophages, the expression of TIMP-1 could be much greater than that of TIMP-3. Therefore, it is possible that in those cells, the significance of ADAM10 in TNF-α shedding could be reduced by the abundance of TIMP-1. In an analogy of macrophages, the expression of TIMP-1 could be more abundant than that of TIMP-3 in articular chondrocytes, which might explain the predominance of ADAM17 over ADAM10 in TNF-α shedding in the cells.

Vascular endothelial cells have been shown to secrete TNF-α in vitro and in vivo. In spinal cord injury in rats, vascular endothelial cells as well as neurons and glial cells expressed TNF-α around the injury site (Yan et al. 2001). Since the inhibition of TNF-α led to the suppression of inflammation and tissue injury in spinal cord injury in mice (Genovese et al. 2008), TNF-α could play an important role in this pathology. Considering the result with UV♀2 cells, it seems possible in that condition that TNF-α is expressed by the endothelial cells and processed by both ADAM10 and ADAM17. The involvement of ADAM10 in the actual human vasculitis has been suggested by the result of immunostaining performed on the skin tissues from a patient with Henoch-Schönlein purpura. In the acute phase of this disease, TNF-α increases in serum and endothelial cells are likely the source of this cytokine (Besbas et al. 1997; Ha 2005). Therefore, the observation that endothelial cells express TNF-α and ADAM10 together convincingly indicates that ADAM10 could play a significant role in the release of TNF-α in the disease. Furthermore, the fact that human endothelial cells were intensely stained for ADAM10 (Fig. 6E) would suggest that those cells have a capacity to express the proteinase at significant levels. Considering this, ADAM10 could indeed be a major TNF-α sheddase in certain pathologies in which endothelial cells express TNF-α.

Although ADAM9 could process TNF-α and is abundantly expressed in macrophages, we could not find any evidence for its involvement in TNF-α shedding. The reason for this was not clarified in this study. Since ADAM9 is not suppressed by TIMPs (Amour et al. 2002), other endogenous inhibitor(s) for ADAM9 might have been expressed and prevented it from shedding.

The result of this study suggested a possibility that ADAM10 can be a major TNF-α sheddase in certain cell types or certain biological situations. As shown in macrophages, ADAM17 is the principal sheddase for TNF-α in certain cell types when ADAM10 activity is inhibited by TIMP-1. In fact, even in macrophages, ADAM10 can be a major sheddase when TIMP-1 expression is reduced for some reason. Thus, we have shown some evidence that both ADAM10 and ADAM17 can work as a sheddase for TNF-α. Their significance in the shedding may be determined by various factors, such as cell types, their expression levels, and the abundance of TIMPs. Since TNF-α is profoundly involved in various biological events, the present observation could be of some help in understanding the kinetics of mobilization of the cytokine.

Acknowledgements

The authors thank Dr. Sunao Takeshita for providing CMG14-12 and pMX-IRES-bsr and Dr. Motoharu Seiki for the expression vectors for MT1-MMP, MT2-MMP, MT3-MMP, MT4-MMP, MT5-MMP, and MT6-MMP. This work was supported in part by a Grant-in-Aid for Young Scientists (B) from the Japan Society for the Promotion of Science to A.H.

References

Alexopoulou, L., Pasparakis, M., and Kollias, G. 1997. A murine transmembrane tumor necrosis factor (TNF) transgene induces arthritis by cooperative p55/p75 TNF receptor signaling. Eur. J. Immunol. **27**(10): 2588–2592. doi:10.1002/eji.1830271018. PMID:9368614.

Amour, A., Slocombe, P.M., Webster, A., Butler, M., Knight, C.G., Smith, B.J., et al. 1998. TNF-alpha converting enzyme (TACE) is inhibited by TIMP-3. FEBS Lett. **435**(1): 39–44. doi:10.1016/S0014-5793(98)01031-X. PMID:9755855.

Amour, A., Knight, C.G., Webster, A., Slocombe, P.M., Stephens, P.E., Knäuper, V., et al. 2000. The in vitro activity of ADAM-10 is inhibited by TIMP-1 and TIMP-3. FEBS Lett. **473**(3): 275–279. doi:10.1016/S0014-5793(00)01528-3. PMID:10818225.

Amour, A., Knight, C.G., English, W.R., Webster, A., Slocombe, P.M., Knäuper, V., et al. 2002. The enzymatic activity of ADAM8 and ADAM9 is not regulated by TIMPs. FEBS Lett. **524**(1-3): 154–158. doi:10.1016/S0014-5793(02)03047-8. PMID:12135759.

Bell, J.H., Herrera, A.H., Li, Y., and Walcheck, B. 2007. Role of ADAM17 in the ectodomain shedding of TNF-α and its receptors by neutrophils and macrophages. J. Leukoc. Biol. **82**(1): 173–176. doi:10.1189/jlb.0307193. PMID:17510296.

Besbas, N., Saatci, U., Ruacan, S., Ozen, S., Sungur, A., Bakkaloglu, A., and Elnahas, A.M. 1997. The role of cytokines in Henoch Schonlein purpura. Scand. J. Rheumatol. **26**(6): 456–460. PMID:9433407.

Black, R.A., Rauch, C.T., Kozlosky, C.J., Peschon, J.J., Slack, J.L., Wolfson, M.F., et al. 1997. A metalloproteinase disintegrin that releases tumour-necrosis factor-alpha from cells. Nature. **385**(6618): 729–733. doi:10.1038/385729a0. PMID:9034190.

Brennan, F.M., Chantry, D., Jackson, A., Maini, R., and Feldmann, M. 1989. Inhibitory effect of TNF alpha antibodies on synovial cell interleukin-1 production in rheumatoid arthritis. Lancet. **2**(8657): 244–247. doi:10.1016/S0140-6736(89)90430-3. PMID:2569055.

Buxbaum, J.D., Liu, K.N., Luo, Y., Slack, J.L., Stocking, K.L., Peschon, J.J., et al. 1998. Evidence that tumor necrosis factor alpha converting enzyme is involved in regulated alpha-secretase cleavage of the Alzheimer amyloid protein precursor. J. Biol. Chem. **273**(43): 27765–27767. doi:10.1074/jbc.273.43.27765. PMID:9774383.

Carswell, E.A., Old, L.J., Kassel, R.L., Green, S., Fiore, N., and Williamson, B. 1975. An endotoxin-induced serum factor that

causes necrosis of tumors. Proc. Natl. Acad. Sci. U.S.A. **72**(9): 3666–3670. doi:10.1073/pnas.72.9.3666. PMID:1103152.

Chesneau, V., Becherer, J.D., Zheng, Y., Erdjument-Bromage, H., Tempst, P., and Blobel, C.P. 2003. Catalytic properties of ADAM19. J. Biol. Chem. **278**(25): 22331–22340. doi:10.1074/jbc.M302781200. PMID:12682046.

Coeshott, C., Ohnemus, C., Pilyavskaya, A., Ross, S., Wieczorek, M., Kroona, H., et al. 1999. Converting enzyme-independent release of tumor necrosis factor alpha and IL-1beta from a stimulated human monocytic cell line in the presence of activated neutrophils or purified proteinase 3. Proc. Natl. Acad. Sci. U.S.A. **96**(11): 6261–6266. doi:10.1073/pnas.96.11.6261. PMID:10339575.

Condon, T.P., Flournoy, S., Sawyer, G.J., Baker, B.F., Kishimoto, T.K., and Bennett, C.F. 2001. ADAM17 but not ADAM10 mediates tumor necrosis factor-alpha and L-selectin shedding from leukocyte membranes. Antisense Nucleic Acid Drug Dev. **11**(2): 107–116. doi:10.1089/108729001750171353. PMID:11334139.

Cseh, K., and Beutler, B. 1989. Alternative cleavage of the cachectin/tumor necrosis factor propeptide results in a larger, inactive form of secreted protein. J. Biol. Chem. **264**(27): 16256–16260. PMID:2777790.

Fernandes, J.C., Martel-Pelletier, J., and Pelletier, J.P. 2002. The role of cytokines in osteoarthritis pathophysiology. Biorheology. **39**(1–2): 237–246. PMID:12082286.

Fiuza, C., Bustin, M., Talwar, S., Tropea, M., Gerstenberger, E., Shelhamer, J.H., and Suffredini, A.F. 2003. Inflammation-promoting activity of HMGB1 on human microvascular endothelial cells. Blood. **101**(7): 2652–2660. doi:10.1182/blood-2002-05-1300. PMID:12456506.

Freyer, D., Manz, R., Ziegenhorn, A., Weih, M., Angstwurm, K., Döcke, W.D., et al. 1999. Cerebral endothelial cells release TNF-alpha after stimulation with cell walls of *Streptococcus pneumoniae* and regulate inducible nitric oxide synthase and ICAM-1 expression via autocrine loops. J. Immunol. **163**(8): 4308–4314. PMID:10510370.

Fukui, N., Ikeda, Y., Ohnuki, T., Hikita, A., Tanaka, S., Yamane, S., et al. 2006. Pro-inflammatory cytokine tumor necrosis factor-α induces bone morphogenetic protein-2 in chondrocytes via mRNA stabilization and transcriptional up-regulation. J. Biol. Chem. **281**(37): 27229–27241. doi:10.1074/jbc.M603385200. PMID:16835229.

Genovese, T., Mazzon, E., Crisafulli, C., Di Paola, R., Muià, C., Esposito, E., et al. 2008. TNF-alpha blockage in a mouse model of SCI: evidence for improved outcome. Shock. **29**(1): 32–41. PMID:17621255.

Gomez, D.E., Alonso, D.F., Yoshiji, H., and Thorgeirsson, U.P. 1997. Tissue inhibitors of metalloproteinases: structure, regulation and biological functions. Eur. J. Cell Biol. **74**(2): 111–122. PMID:9352216.

Ha, T.S. 2005. The role of tumor necrosis factor-alpha in Henoch-Schonlein purpura. Pediatr. Nephrol. **20**(2): 149–153. doi:10.1007/s00467-004-1726-3. PMID:15627167.

Haro, H., Crawford, H.C., Fingleton, B., Shinomiya, K., Spengler, D.M., and Matrisian, L.M. 2000. Matrix metalloproteinase-7-dependent release of tumor necrosis factor-alpha in a model of herniated disc resorption. J. Clin. Invest. **105**(2): 143–150. doi:10.1172/JCI7091. PMID:10642592.

Hikita, A., Kadono, Y., Chikuda, H., Fukuda, A., Wakeyama, H., Yasuda, H., et al. 2005. Identification of an alternatively spliced variant of Ca^{2+}-promoted Ras inactivator as a possible regulator of RANKL shedding. J. Biol. Chem. **280**(50): 41700–41706. doi:10.1074/jbc.M507000200. PMID:16234249.

Hikita, A., Yana, I., Wakeyama, H., Nakamura, M., Kadono, Y., Oshima, Y., et al. 2006. Negative regulation of osteoclastogenesis by ectodomain shedding of receptor activator of NF-kappaB ligand. J. Biol. Chem. **281**(48): 36846–36855. doi:10.1074/jbc.M606656200. PMID:17018528.

Horiuchi, K., Kimura, T., Miyamoto, T., Takaishi, H., Okada, Y., Toyama, Y., and Blobel, C.P. 2007. Cutting edge: TNF-α-converting enzyme (TACE/ADAM17) inactivation in mouse myeloid cells prevents lethality from endotoxin shock. J. Immunol. **179**(5): 2686–2689. PMID:17709479.

Kitamura, T. 1998. New experimental approaches in retrovirus-mediated expression screening. Int. J. Hematol. **67**(4): 351–359. doi:10.1016/S0925-5710(98)00025-5. PMID:9695408.

Kobayashi, M., Plunkett, J.M., Masunaka, I.K., Yamamoto, R.S., and Granger, G.A. 1986. The human LT system. XII. Purification and functional studies of LT and "TNF-like" LT forms from a continuous human T cell line. J. Immunol. **137**(6): 1885–1892. PMID:2427583.

Koike, H., Tomioka, S., Sorimachi, H., Saido, T.C., Maruyama, K., Okuyama, A., et al. 1999. Membrane-anchored metalloprotease MDC9 has an alpha-secretase activity responsible for processing the amyloid precursor protein. Biochem. J. **343**(Pt. 2): 371–375. doi:10.1042/0264-6021:3430371. PMID:10510302.

Kriegler, M., Perez, C., DeFay, K., Albert, I., and Lu, S.D. 1988. A novel form of TNF/cachectin is a cell surface cytotoxic transmembrane protein: ramifications for the complex physiology of TNF. Cell. **53**(1): 45–53. doi:10.1016/0092-8674(88)90486-2. PMID:3349526.

Küsters, S., Tiegs, G., Alexopoulou, L., Pasparakis, M., Douni, E., Künstle, G., et al. 1997. In vivo evidence for a functional role of both tumor necrosis factor (TNF) receptors and transmembrane TNF in experimental hepatitis. Eur. J. Immunol. **27**(11): 2870–2875. doi:10.1002/eji.1830271119. PMID:9394812.

Lammich, S., Kojro, E., Postina, R., Gilbert, S., Pfeiffer, R., Jasionowski, M., et al. 1999. Constitutive and regulated alpha-secretase cleavage of Alzheimer's amyloid precursor protein by a disintegrin metalloprotease. Proc. Natl. Acad. Sci. U.S.A. **96**(7): 3922–3927. doi:10.1073/pnas.96.7.3922. PMID:10097139.

Li, Y.M., Lai, M.T., Xu, M., Huang, Q., DiMuzio-Mower, J., Sardana, M.K., et al. 2000. Presenilin 1 is linked with gamma-secretase activity in the detergent solubilized state. Proc. Natl. Acad. Sci. U.S.A. **97**(11): 6138–6143. doi:10.1073/pnas.110126897. PMID:10801983.

Lunn, C.A., Fan, X., Dalie, B., Miller, K., Zavodny, P.J., Narula, S.K., and Lundell, D. 1997. Purification of ADAM 10 from bovine spleen as a TNFalpha convertase. FEBS Lett. **400**(3): 333–335. doi:10.1016/S0014-5793(96)01410-X. PMID:9009225.

Mahmoodi, M., Sahebjam, S., Smookler, D., Khokha, R., and Mort, J.S. 2005. Lack of tissue inhibitor of metalloproteinases-3 results in an enhanced inflammatory response in antigen-induced arthritis. Am. J. Pathol. **166**(6): 1733–1740. PMID:15920158.

McGeehan, G.M., Becherer, J.D., Bast, R.C., Jr., Boyer, C.M., Champion, B., Connolly, K.M., et al. 1994. Regulation of tumour necrosis factor-alpha processing by a metalloproteinase inhibitor. Nature. **370**(6490): 558–561. doi:10.1038/370558a0. PMID:8052311.

Mohler, K.M., Sleath, P.R., Fitzner, J.N., Cerretti, D.P., Alderson, M., Kerwar, S.S., et al. 1994. Protection against a lethal dose of endotoxin by an inhibitor of tumour necrosis factor processing. Nature. **370**(6486): 218–220. doi:10.1038/370218a0. PMID:8028669.

Moss, M.L., Jin, S.L., Milla, M.E., Bickett, D.M., Burkhart, W., Carter, H.L., et al. 1997. Cloning of a disintegrin metalloproteinase that processes precursor tumour-necrosis factor-alpha. Nature. **385**(6618): 733–736. doi:10.1038/385733a0. PMID:9034191.

Mueller, C., Corazza, N., Trachsel-Løseth, S., Eugster, H.P., Bühler-Jungo, M., Brunner, T., and Imboden, M.A. 1999. Noncleavable transmembrane mouse tumor necrosis factor-α (TNF-α) mediates effects distinct from those of wild-type TNF-α in vitro and in vivo. J. Biol. Chem. **274**(53): 38112–38118. doi:10.1074/jbc.274.53.38112. PMID:10608881.

Nilsen, E.M., Johansen, F.E., Jahnsen, F.L., Lundin, K.E., Scholz, T., Brandtzaeg, P., and Haraldsen, G. 1998. Cytokine profiles of cultured microvascular endothelial cells from the human intestine. Gut, **42**(5): 635–642. PMID:9659156.

Pelletier, J.P., Martel-Pelletier, J., and Abramson, S.B. 2001. Osteoarthritis, an inflammatory disease: potential implication for the selection of new therapeutic targets. Arthritis Rheum. **44**(6): 1237–1247. doi:10.1002/1529-0131(200106)44:6<1237::AID-ART214>3.0.CO;2-F. PMID:11407681.

Reinecker, H.C., Steffen, M., Witthoeft, T., Pflueger, I., Schreiber, S., MacDermott, R.P., and Raedler, A. 1993. Enhanced secretion of tumour necrosis factor-alpha, IL-6, and IL-1 beta by isolated lamina propria mononuclear cells from patients with ulcerative colitis and Crohn's disease. Clin. Exp. Immunol. **94**(1): 174–181. PMID:8403503.

Schlöndorff, J., Lum, L., and Blobel, C.P. 2001. Biochemical and pharmacological criteria define two shedding activities for TRANCE/OPGL that are distinct from the tumor necrosis factor alpha convertase. J. Biol. Chem. **276**(18): 14665–14674. doi:10.1074/jbc.M010741200. PMID:11278735.

Schneider, P., Holler, N., Bodmer, J.L., Hahne, M., Frei, K., Fontana, A., and Tschopp, J. 1998. Conversion of membrane-bound Fas(CD95) ligand to its soluble form is associated with downregulation of its proapoptotic activity and loss of liver toxicity. J. Exp. Med. **187**(8): 1205–1213. doi:10.1084/jem.187.8.1205. PMID:9547332.

Schulte, M., Reiss, K., Lettau, M., Maretzky, T., Ludwig, A., Hartmann, D., et al. 2007. ADAM10 regulates FasL cell surface expression and modulates FasL-induced cytotoxicity and activation-induced cell death. Cell Death Differ. **14**(5): 1040–1049. PMID:17290285.

Selkoe, D.J. 1991. The molecular pathology of Alzheimer's disease. Neuron, **6**(4): 487–498. doi:10.1016/0896-6273(91)90052-2. PMID:1673054.

Steffen, M., Abboud, M., Potter, G.K., Yung, Y.P., and Moore, M.A. 1989. Presence of tumour necrosis factor or a related factor in human basophil/mast cells. Immunology, **66**(3): 445–450. PMID:2703257.

Tracey, K.J., Fong, Y., Hesse, D.G., Manogue, K.R., Lee, A.T., Kuo, G.C., et al. 1987. Anti-cachectin/TNF monoclonal antibodies prevent septic shock during lethal bacteraemia. Nature, **330**(6149): 662–664. doi:10.1038/330662a0. PMID:3317066.

Vassar, R., Bennett, B.D., Babu-Khan, S., Kahn, S., Mendiaz, E.A., Denis, P., et al. 1999. Beta-secretase cleavage of Alzheimer's amyloid precursor protein by the transmembrane aspartic protease BACE. Science, **286**(5440): 735–741. doi:10.1126/science.286.5440.735. PMID:10531052.

Verrier, S., Hogan, A., McKie, N., and Horton, M. 2004. ADAM gene expression and regulation during human osteoclast formation. Bone, **35**(1): 34–46. doi:10.1016/j.bone.2003.12.029. PMID:15207739.

Yamamoto, A., Miyazaki, T., Kadono, Y., Takayanagi, H., Miura, T., Nishina, H., et al. 2002. Possible involvement of IκB kinase 2 and MKK7 in osteoclastogenesis induced by receptor activator of nuclear factor κB ligand. J. Bone Miner. Res. **17**(4): 612–621. doi:10.1359/jbmr.2002.17.4.612. PMID:11918218.

Yan, P., Li, Q., Kim, G.M., Xu, J., Hsu, C.Y., and Xu, X.M. 2001. Cellular localization of tumor necrosis factor-alpha following acute spinal cord injury in adult rats. J. Neurotrauma, **18**(5): 563–568. doi:10.1089/089771501300227369. PMID:11393259.

Zheng, Y., Saftig, P., Hartmann, D., and Blobel, C. 2004. Evaluation of the contribution of different ADAMs to tumor necrosis factor alpha (TNF-alpha) shedding and of the function of the TNF-alpha ectodomain in ensuring selective stimulated shedding by the TNF-alpha convertase (TACE/ADAM17). J. Biol. Chem. **279**(41): 42898–42906. doi:10.1074/jbc.M403193200. PMID:15292243.

J Cancer Res Clin Oncol (2010) 136:323–331
DOI 10.1007/s00432-009-0688-z

ORIGINAL PAPER

Aberrant $p16^{INK4a}$ methylation is a frequent event in colorectal cancers: prognostic value and relation to mRNA expression and immunoreactivity

Hiroyuki Mitomi · Naoshi Fukui · Nobuho Tanaka · Hideki Kanazawa · Tsuyoshi Saito · Takashi Matsuoka · Takashi Yao

Received: 3 September 2008 / Accepted: 14 September 2009 / Published online: 25 September 2009

Abstract
Purpose Aberrant $p16^{INK4a}$ promoter methylation is common in colorectal cancer (CRC), but its clinicopathological significance remains controversial. The present study was therefore conducted to analyze $p16^{INK4a}$ methylation and its relationship to clinicopathological features, mRNA levels and immunoreactivity in a series of lesions.
Methods $p16^{INK4a}$ methylation was assessed for normal mucosa ($n = 30$) and CRC samples ($n = 212$) by methylation-specific real-time quantitative PCR, and $p16^{INK4a}$ expression by immunostaining in formalin-fixed paraffin-embedded specimens. In addition, fresh DNA ($n = 61$) was analyzed for relationships to $p16^{INK4a}$ mRNA by reverse-transcription PCR.
Results The $p16^{INK4a}$ methylation index of normal mucosa samples ranged from 0 to 2% (mean, 0.23%; median, 0.02%), while the values for tumor samples varied widely from 0 to 100% (mean, 25.7%; median, 7.1%), the difference being statistically significant ($P < 0.001$). Of 151 paraffin-embedded CRC tissue samples, 51 (34%), 54 (36%), and 46 (30%) were classified as low, intermediate, and high for aberrant methylation of $p16^{INK4a}$. High $p16^{INK4a}$ methylation was significantly associated with large tumor size ($P = 0.025$). Patients with higher methylation further showed more frequent recurrence as compared with the low-methylation group, and shortened cancer-related survival (Hazard ratio [HR], 3.379; $P < 0.001$) and recurrence-free survival (HR, 3.962; $P < 0.001$ on multivariate analysis). A significant inverse relationship was apparent between the $p16^{INK4a}$ methylation and immunoreactivity ($P = 0.017$). A similar tendency was also observed for the methylation status and the mRNA level ($P = 0.195$).
Conclusions We conclude that $p16^{INK4a}$ methylation results in transcriptional silencing and defines a group of CRCs with a poor prognosis.

Keywords $p16^{INK4a}$ · Methylation · Colorectal cancer · Prognosis

H. Mitomi (✉) · T. Saito · T. Matsuoka · T. Yao
Department of Human Pathology,
Juntendo University School of Medicine,
2-1-1 Hongo, Bunkyo-ku, Tokyo 113-8421, Japan
e-mail: hmitomi@juntendo.ac.jp

N. Fukui · N. Tanaka
Department of Pathomechanisms, Clinical Research Center,
National Hospital Organization, Sagamihara Hospital,
Sagamihara, Japan

H. Kanazawa
Department of Surgery,
National Hospital Organization, Sagamihara Hospital,
Sagamihara, Japan

Introduction

Abnormal patterns of DNA hypermethylation are common in human tumors, promoter-associated CpG island regions being involved in many of the affected neoplastic cells (Baylin et al. 1998). In colorectal cancers, as with other tumors, aberrant promoter methylation frequently results in silencing of tumor suppressor genes such as APC (Derks et al. 2006; Iacopetta et al. 2006), O^6MGMT (Derks et al. 2006) and hMLH1 (Toyota et al. 1999; Shannon and Iacopetta. 2001; Van Rijnsoever et al. 2002; Ward et al. 2003; Iacopetta et al. 2006; Ogino et al. 2006). $p16^{INK4a}$ (p16) is located on chromosome 9p21 that exerts a negative effect on cell cycle progression at the G1/S checkpoint by

inhibition of binding of cyclin D/CDK4 or cyclin D/CDK6 complexes in the Rb pathway (Serrano et al. 1995). Inactivation of p16, therefore, can result in a cellular inability to activate the Rb gene, with resultant loss of the cellular capacity to block cell cycle progression (Weinberg 1995). p16 mutations that lead to inactivation are found in many tumor types (Kamb et al. 1994; Nobori et al. 1994), but generally are lacking in colorectal cancers (Burri et al. 2001). Homozygous deletions, described in colon cancer cell lines (Guan et al. 1999; Burri et al. 2001) and hypermethylation of the promoter are alternative major mechanisms of p16 inactivation, which occurs in 40% of colon cancers while being absent in normal colonic epithelium in an earlier report (Herman et al. 1995).

The aim of the present study was to investigate aberrant p16 promoter methylation in a series of sporadic colorectal cancers and assess any association with clinicopathological features and prognostic relevance. In addition, relationships between the p16 methylation status and mRNA levels or protein expression were examined.

Materials and methods

Patients and materials

The subjects of our study were a series of 151 patients diagnosed with and undergoing surgery for colorectal carcinoma at the National Hospital Organization Sagamihara Hospital between April 1996 and March 2001. Surgically resected specimens were fixed in 10% formalin and embedded in paraffin wax, according to routine procedures, and sections were cut and stained with hematoxylin and eosin (H&E). Patients with familial polyposis coli, hereditary non-polyposis colorectal carcinoma, multiple colorectal carcinomas or inflammatory bowel disease, or those who had died within 30 days of surgery were not included in the analysis. No patient received initial chemotherapy or radiotherapy. The 151 patients comprised 95 males and 56 females, with a mean age of 65.8 years (median, 67 years; range, 39–86).

For biochemical studies of p16 transcription, fresh tumor tissues and corresponding normal mucosa distant from the tumor were obtained from 61 patients (36 males and 25 females; mean/median age, 69.8/70.5 years [range, 36–87]) between February and June 2007. Tissue blocks were prepared immediately after surgical resection, snap-frozen in liquid nitrogen, and stored at −80°C. For immunohistochemistry, another tissue block obtained simultaneously was fixed in 10% formalin and embedded in paraffin wax. Informed consent was obtained from all patients and the study was approved by our hospital's clinical research and ethics committee.

Pathological review

Slides stained with H&E were examined by an experienced gastrointestinal pathologist (HM). Proximal cancers were classified as tumors proximal to the splenic flexure and the remaining tumors were defined as distal. The depth of invasion (pT category), lymph node involvement (pN category), and pathological staging of all surgically resected tumors were assessed according to the UICC/TNM classification (International Union Against Cancer 1997). Out of 151 patients, 70 were diagnosed pathologically to have TNM stage II lesions, 57 stage III and 24 stage IV.

Adjuvant chemotherapy and follow-up

In 48 out of the 57 stage III patients, postoperative oral administration of 5-fluorouracil (5-FU) derivatives was given for at least 1 year. In 13 patients out of 24 with stage IV cases, 5-FU plus mitomycin C or leukovorin was applied by intravenous infusion biweekly after surgery. All patients were followed up regularly by physical and blood examinations with mandatory screening by colonoscopy, ultrasound, computed tomography or magnetic resonance imaging. Locoregional recurrence was defined as a tumor occurring at the anastomosis or in the locoregional lymph nodes, retroperitoneum or pelvic wall. Distant recurrences were defined as tumor manifestations outside the site of resection in the peritoneal cavity or other organs. The patients were observed for more than 5 years, and the median duration of follow-up was 79 months (range, 60–123), for the survivors were alive at the date of their last visit ($n = 87$).

DNA and RNA extraction

Genomic DNA was extracted from five 10-μm-thick formalin-fixed paraffin-embedded sections of the 151 tumors (one paraffin block representing the tumor center without normal mucosa) and 20 normal tissues (one paraffin block distant from the tumor), and from frozen sections of 61 tumors and 10 normal tissues using a DNeasy kit (Qiagen, Valencia, CA, USA), according to the manufacturer's instructions. In addition, DNA was extracted from a colon cancer cell line SW480 (American Type Culture Collection), in which the promoter of the p16 gene is reported to be fully methylated (Herman et al. 1995), as a positive control. DNA from peripheral blood leukocytes of a healthy volunteer was employed as a negative control for bisulfite conversion, DNA recovery, and PCR reaction.

Total RNA was extracted from frozen sections of 43 tumor tissues using a RNeasy Micro kit (Qiagen) with DNaseI (Qiagen), according to the manufacturer's protocol.

Bisulfite modification and real-time quantitative methylation-specific PCR

Bisulfite modification was conducted using an EZ DNA Methylation-Gold Kit (Zymo Research, Orange, CA, USA). Two micrograms of DNA was treated with sodium bisulfite following the manufacturer's recommendations and amplified using specifically designed primers for methylated and unmethylated p16 sequences and a *Taqman* probe. The sense and antisense primers for the methylated sequence were 5′-GTTATTAGAGGGTGGGGCGGATCG CG-3′ and 5′-CGAACCGCGACCGTAACCA-3′, respectively. These primers were used in conjunction with a *Taqman* probe [5′-(FAM)-AGTAGTATGGAGTCGGCGGCG GG-(TAMRA)-3′]. The sense and antisense primers for the unmethylated sequence were 5′-GGTTATTAGAGGGTG GGGTGGATTGTG-3′ and 5′-CCCAACCCCAAACCAC AACCATATCC-3′, respectively, used in conjunction with another *Taqman* probe [5′-(FAM)-AGGTAGTGGGTG GTGGGGAGTAGTATGGAGTTG-(TAMRA)-3′].

Real-time quantitative methylation-specific PCR (MSP) was performed with Premix Ex Taq (Takara Bio, Shiga, Japan) on a LightCycler (Roche Diagnostics, Basel, Switzerland). The PCR protocol was the same for methylated and unmethylated p16, *i.e.*, 95°C for 10 min to activate *Taq* polymerase, then 60 cycles of 95°C for 10 s and 68°C for 30 s. All PCR runs included separate reactions with templates from p16-fully methylated and the unmethylated control DNA, as well as with no template. The methylation index (MI; percentage) in a sample was calculated according to the equation: (concentration of methylated p16 sequence/concentrations of methylated plus unmethylated p16 sequence) × 100 (Kim et al. 2005).

Reverse transcription real-time quantitative PCR analysis

One microgram of total RNA was employed to synthesize cDNA using Sensiscript reverse transcriptase (Qiagen). The cDNA was then used for real-time quantitative PCR on a LightCycler. The primer pairs located in exons 1α and 2 with flanking intron 1 of the p16 gene were 5′-GAGCAG CATGGAGCCTTC-3′ and 5′-ACCGTAACTATTCGGT GCGTT-3′. The probe sequence for p16 was 5′-(FAM)-TA GAGGAGGTGCGGGCGCTGC-(TAMRA)-3′. The PCR protocol was as follows: 95°C for 10 min to activate *Taq* polymerase, then 60 cycles of 95°C for 10 s and 56°C for 30 s. Glyceraldehyde-3-phosphate dehydrogenase (GAPDH) gene expression was used as an internal standard, its cDNA being amplified with the following primers: 5′-CAGGGA CTCCCCAGCAGT-3′ and 5′-GGCATTGCCCTCAACG ACCA-3′. These primers were used in conjunction with SYBR Green I. The PCR protocol was as follows: 95°C for 10 min to activate *Taq* polymerase, then 40 cycles of 95°C for 10 s, 60°C for 15 s, and 72°C for 6 s. For each sample, the level of cDNA was normalized to the expression of GAPDH. SYBR Premix Ex Taq (takara Bio, Shiga, Japan) was used for the reaction.

Immunohistochemistry

We randomly selected 25 blocks from 25 tumor samples, which were prepared for immunohistochemical analysis. Immunostaining was performed with DakoCytomation Autostainer Instruments (DakoCytomation, Kyoto, Japan). Briefly, 4-μm-thick tissue sections were dewaxed in xylene and rehydrated in decreasing concentrations of ethanol. Endogeneous peroxidase activity was blocked by incubation with Peroxidase-Blocking Solution (DakoCytomation) for 5 min. Antigen retrieval consisted of autoclave treatment of sections for 30 min in Epitope Retrieval Solution. The primary antibody employed was monoclonal anti-p16 (E6H4, prediluted, DakoCytomation), with incubation for 30 min at room temperature. Using an Envision Kit, the slides were incubated with horseradish peroxidase-labeled polymer conjugated with secondary antibody for 30 min and then with Substrate-Chromogen (diaminobenzidine) Solution, followed by light counterstaining with Mayer's hematoxylin. Sections of a squamous cell carcinoma of the esophagus with known positivity for p16 were used as external positive controls. For negative controls, the primary antibodies were omitted.

Assessment of immunostaining

Image analysis using Image-Pro Plus (Version 5.1, Media Cybernetics Inc., Silver Spring, MD, USA) was performed on p16 immunostained slides; five images were captured in each case from the areas of their highest immunoreactivity at 25× magnification with a Digital Microscopy Camera (DP50-CU, Olympus Co., Tokyo, Japan) and processed with Viewfinder Lite software (Version 1.0, Pixera Corp., San Jose, CA, USA) and Adobe Photoshop software programs (Version 7.0, Adobe Photoshop Inc., San Jose, CA, USA). Distinct nuclear staining was considered to be positive, regardless of the staining intensity. When there was cytoplasmic staining, a nucleus was regarded as positive if its staining intensity equaled or exceeded that of the surrounding cytoplasm. In negative cases, sporadically decorated stromal fibroblasts served as convenient internal controls. Finally, p16-immunolabeling indices were obtained by calculating the percentage of the total area of positively stained tumor cells per whole lesion.

Statistical analysis

Categorical analysis of variables was performed using either the chi-squared test (with Yates' correction) or the

Fisher's exact test, as appropriate. Continuous data were compared with the Mann–Whitney *U*-test or Kruskal–Wallis test. Survival curves were generated by the Kaplan–Meier method. Cancer-related survival time was measured from the date of surgery to the end of follow-up or death due to colorectal cancer or other causes. Recurrence-free survival time was defined as the time from surgery to recurrent disease (alive) or death with or without recurrence. The patients who had metastases diagnosed at surgery or had incomplete resection were excluded from analyses of recurrence-free survival ($n = 127$). Associations between MI and clinicopathological features, and survival were examined using univariate and multivariate Cox's regression analyses. In the Cox's multivariate analysis, a step-wise backward variable elimination method was used with an entry limit of $P < 0.1$ and a removal limit of $P \geq 0.05$. A P value of less than 0.05 was considered statistically significant. All statistical analyses were carried out using StatView for Windows Version 5.0 (SAS Institute Inc., Cary, NC, USA).

Results

p16 MI in normal and tumor tissue samples

The p16 MI values for normal mucosa samples ($n = 30$) ranged from 0 to 2% (mean, 0.23%; median, 0.02%), while for tumor samples ($n = 212$) they varied widely from 0 to 100% (mean, 25.7%; median, 7.1%), the difference being statistically significant ($P < 0.001$). Tumor cases were classified into three categories as follows: low (MI $\leq$ 2%), intermediate (2 < MI $\leq$ 40%), and high (MI > 40%) aberrant p16 methylation groups, accounting for 51 (34%), 54 (36%), and 46 (30%), respectively, of the 151 paraffin-embedded tumor samples.

Associations between the p16 methylation status and clinicopathological features

High aberrant p16 methylation was significantly associated with large tumor size ($P = 0.025$), but not with other clinicopathological features (Table 1).

Table 1 Associations between p16 methylation status and clinicopathological features

Variable	Aberrant p16 methylation			*P* value
	Low ($n = 51$)	Intermediate ($n = 54$)	High ($n = 46$)	
Sex				
Male	29	37	29	NS
Female	22	17	17	
Age				
<60 years	14	14	12	NS
≥60 years	37	40	34	
Size				
<5.0 cm	28	39	23	0.025*
≥5.0 cm	23	15	23	
Location				
Proximal	12	22	16	NS
Distal	39	32	30	
Differentiation				
Well	22	26	25	NS
Moderate	27	22	19	
Poor	2	6	2	
pT category				
pT3	49	52	42	NS
pT4	2	2	4	
pN category				
pN0	25	28	23	NS
pN1	22	16	16	
pN2	4	10	7	
TNM stage				
II	22	25	23	NS
III	21	20	16	
IV	8	9	7	

* Intermediate vs. high p16 methylation group

Impact on cancer-related survival

Based on univariate analysis (Table 2), patients with high p16 methylation had significantly worse ($P = 0.002$) survival than those with low or intermediate methylation (Fig. 1a). In addition, tumor differentiation ($P < 0.001$), pT category ($P = 0.003$), pN category ($P < 0.001$) and TNM stage ($P < 0.001$) had significant influence on cancer-related survival. In the Cox's regression model, high methylation group ($P < 0.001$), high pT ($P = 0.013$) and advanced TNM stage ($P < 0.001$) proved to be independent predictors of short cancer-related survival (Table 3).

Impact on recurrence-free survival

Twenty (16%) of 127 patients suffered isolated locoregional recurrence, and 20 (16%) had distant metastases. Patients with intermediate and high p16 methylation (16/127 cases, 13%) showed more frequent locoregional recurrence as compared with the low-methylation group (4/127 cases, 3%; $P = 0.009$). For distant metastases, similar differences were found in patients with metastases to the liver (intermediate and high, 9% vs. low, 2%; $P = 0.019$) and the lung (5% vs. 0%; $P = 0.029$). Other metastatic deposits were found in the peritoneum (2%), bone (1%) and brain (1%), but no significant link was apparent with aberrant methylation.

Table 2 Univariate analysis of clinicopathological features and p16 methylation status with reference to cancer-related survival

Variable	*n*	5-year survival	HR	95% CI	*P* value
Sex					
Male	95	59 (62)	1		
Female	56	34 (61)	0.894	0.526–1.521	NS
Age					
<60 years	40	21 (53)	1		
≥60 years	111	72 (65)	1.415	0.818–2.45	NS
Size					
<5.0 cm	90	56 (62)	1		
≥5.0 cm	61	37 (61)	0.979	0.580–1.651	NS
Location					
Proximal	50	34 (68)	1		
Distal	101	59 (58)	0.773	0.434–1.375	NS
Differentiation					
Well	73	48 (66)	1		
Moderate	68	43 (63)	1.108	0.636–1.929	0.7
Poor	10	2 (20)	4.121	1.848–9.189	<0.001
pT category					
pT3	143	91 (64)	1		
pT4	8	2 (25)	3.585	1.529–8.403	0.003
pN category					
pN0	76	61 (80)	1		
pN1	54	26 (48)	3.366	1.797–6.307	<0.001
pN2	21	6 (29)	4.948	2.411–10.15	<0.001
TNM stage					
II	70	61 (87)	1		
III	57	32 (56)	4.133	1.928–8.858	<0.001
IV	24	0 (0)	26.221	11.74–58.57	<0.001
Aberrant p16 methylation					
Low	51	39 (76)	1		
Intermediate	54	34 (63)	1.819	0.889–3.724	0.102
High	46	20 (62)	2.953	1.487–5.863	0.002

Values in parenthesis are percentages

HR hazard ratio, *CI* confidence interval

NS not significant

On univariate analysis of risk factors for recurrence-free survival (Table 4), patients with high methylation of p16 had a significantly worse prognosis ($P = 0.001$) than those with low or intermediate methylation (Fig. 1b). Furthermore, recurrence-free survival was also strongly related to poor tumor differentiation ($P = 0.01$) and high pN (pN1, $P = 0.002$; pN2, $P < 0.001$). Cox's regression multivariate analysis showed high p16 methylation group (intermediate, $P = 0.04$; high, $P < 0.001$) and advanced TNM stage ($P < 0.001$) to predict short recurrence-free survival (Table 5).

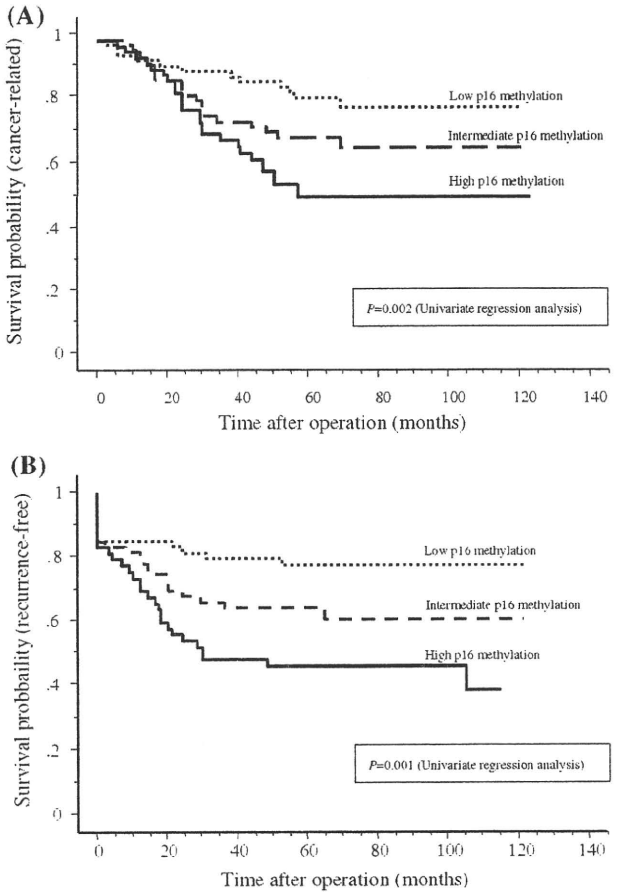

Fig. 1 Cancer-related (**a**) and recurrence-free (**b**) survival cases with reference to aberrant p16 methylation status

Table 3 Multivariate analysis of variables for cancer-related survival in the 151 patients

Variable	HR	95% CI	*P* value
Aberrant p16 methylation			
Low	1		
Intermediate	1.852	0.901–3.81	0.094
High	3.379	1.668–6.843	<0.001
pT category			
pT3	1		
pT4	3.098	1.266–7.585	0.013
TNM stage			
II	1		
III	4.955	2.292–10.71	<0.001
IV	29.33	12.89–66.71	<0.001

HR hazard ratio, *CI* confidence interval

Correlations among p16 methylation status, mRNA level and immunoreactivity in tumor samples

The tumors with high p16 methylation tended to have lower p16 mRNA levels as compared with intermediate or low

Table 4 Univariate analysis of clinicopathological features and p16 methylation status with reference to recurrence-free survival

Variable	*n*	5-year survival	HR	95% CI	*P* value
Sex					
Male	80	55 (67)	1		
Female	47	34 (72)	1.113	0.569–2.178	NS
Age					
<60 years	30	20 (67)	1		
≥60 years	97	69 (71)	1.139	0.553–2.346	NS
Size					
<5.0 cm	74	54 (72)	1		
≥5.0 cm	53	35 (66)	0.752	0.398–1.422	NS
Location					
Proximal	43	32 (74)	1		
Distal	84	57 (68)	0.805	0.399–1.624	NS
Differentiation					
Well	65	45 (69)	1		
Moderate	55	42 (76)	0.723	0.359–1.455	0.364
Poor	7	2 (28)	3.666	1.365–9.842	0.01
pT category					
pT3	122	87 (71)	1		
pT4	5	2 (40)	3.212	0.985–10.48	0.053
pN category					
pN0	70	59 (84)	1		
pN1	43	24 (56)	3.341	1.589–7.025	0.002
pN2	14	6 (43)	4.853	1.944–12.12	<0.001
Aberrant p16 methylation					
Low	51	39 (76)	1		
Intermediate	54	32 (59)	1.939	0.959–3.921	0.065
High	46	18 (39)	3.121	1.584–6.15	0.001

Values in parenthesis are percentages

HR hazard ratio, *CI* confidence interval

NS not significant

Table 5 Multivariate analysis of variables for recurrence-free survival in the 127 patients

Variable	HR	95% CI	*P* value
Aberrant p16 methylation			
Low	1		
Intermediate	2.095	1.033–4.247	0.04
High	3.962	1.987–7.903	<0.001
TNM stage			
II	1		
III	4.545	2.231–9.261	<0.001
IV	325.1	40.8–2589.8	<0.001

HR hazard ratio, *CI* confidence interval

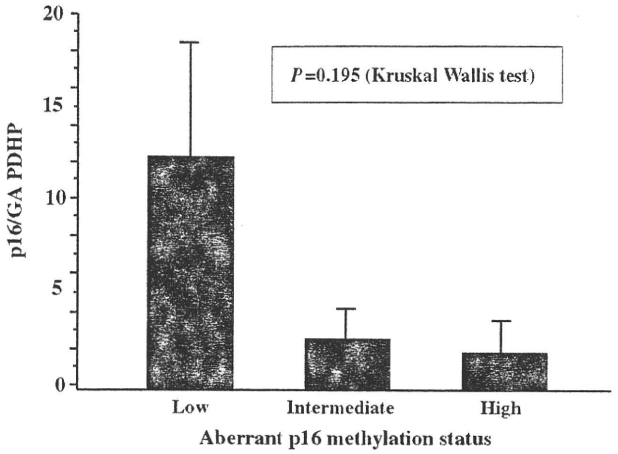

Fig. 2 Associations of p16 mRNA level and aberrant methylation status in tumor samples. The units ascribed to p16 mRNA represent the ratios of p16 to GAPDH on reverse transcription real-time quantitative PCR. Data are means ± standard errors

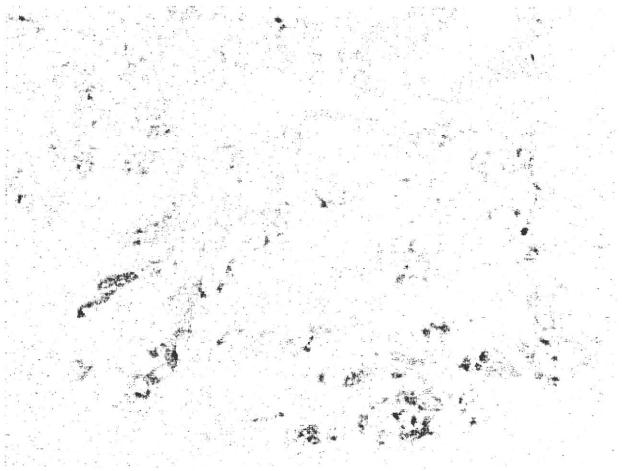

Fig. 3 Example of p16 immunostaining in a colon carcinoma. Note loss of expression in the tumor center and high intensity at the invasive front (original magnification, × 16)

methylation groups, but without any significant difference ($P = 0.195$; Fig. 2).

P16 immunostaining could be clearly discriminated and proved heterogenous, with higher expression commonly seen at invasive fronts (Fig. 3). The p16 immunolabeling indices gradually decreased from low to intermediate and high p16 methylation groups with significant intergroup variation ($P = 0.017$; Fig. 4).

Discussion

In the present study, fluorescence-based real-time quantitative MSP-detected p16 methylation was found to